NAGOYA UNIVERSITY

Tribological properties and the mechanism of ta-C coatings with filtered cathodic vacuum arc deposition at elevated temperature

WooYoung Lee

A thesis submitted in partial fulfillment for the degree of

Doctor of Engineering

in the

DEPARTMENT OF MECHANICAL SCIENCE AND ENGINEERING
GRADUATE SCHOOL OF ENGINEERING

2019

NAGOYA UNIVERSITY

Abstract

DEPARTMENT OF MECHANICAL SCIENCE AND ENGINEERING

GRADUATE SCHOOL OF ENGINEERING

Doctor of Engineering

by Lee

In modern industry, sliding machines are subjected to high temperature environments. Solid lubricating coatings are primarily used to control friction and wear in high temperature environments, where conventional liquid lubricants cannot provide lubrication function due to deterioration and oxidation at high temperature. Solid lubricating coatings include nitrides coatings, carbides coatings, oxides coatings, carbon coatings, soft metals, polymers coatings and lamellar solids. Among these solid lubricating coatings, carbon coatings attract much attention because their excellent mechanical properties and tribological properties, such as low friction, high hardness and high wear resistance. However, the high temperature tribological behaviors and mechanism of carbon coatings are still not clarified yet. Consequently, in this study, tetrahedral amorphous carbon (ta-C) coatings were investigated with

respect to their thermal stability and high temperature tribological properties.

The aim of this study is to clarify effects of substrate bias and elevated temperature during sliding on tribological properties. In addition to investigations the effects of substrate bias on mechanical and micro-structural properties of ta-C coating, ball-on-disk friction tests were conducted in high temperature conditions using Si_3N_4 ball. Besides, friction and wear behavior as a function of different sliding cycles were analyzed to further understand the running-in cycle, wear and formation of carbonaceous transfer layer in high temperature. Additionally, in order to get a comprehensive understanding of the effect of defects in ta-C coating related to running-in cycle, the defects in a designated area on the surface of the ta-C coating were observed and their morphology, structural and tribological behavior were compared with those obtained under high temperature condition.

First, we prepared ta-C coatings by using filtered cathodic vacuum arc (FCVA) deposition. The effect of bias and temperature on properties and tribolgical behavior of the ta-C coating is not clarified. The tribological behaviors of 1 μm of ta-C coatings deposited with different substrate biases of 0 V, -100 V and -300 V were examined under elevated temperature up to 600 ℃. Wear behaviors were found in two distinct ranges in temperature. The variation of the specific wear rate of ta-C coatings in region Ⅰ at 23, 100 and 200 ℃ are affected by abrasive particles of high sp^3 content of

ta-C coatings. In region Ⅱ at 300, 400 and 500 ℃, the transfer layer play a major role in reduction of wear rate as a function of substrate bias.

In the high temperature condition, the high sp^3 content ta-C coating deposited at substrate bias of -100V were found high wear resistance compared to ta-C fabricated at substrate bias of 0 V over testing temperature of 300 ℃. This is caused by the remained hardness and high sp^3 content. We focused on ta-C coating deposited at substrate bias -100 V. Then we clarified wear-in and running-in cycle and role of carbon transferred layer. Ta-C coatings were also subjected to friction tests under 200 ℃ in air with different sliding cycles. The friction coefficient reached 0.02 at steady state after finishing a running-in cycles approximately 2,000 cycles. After reaching the steady state, wear rates of ta-C decreased with increasing number of cycles. The decrease of wear rates was caused to polish defects presented on surface and to form a carbon transferred layer on the counter-part material. The mechanism of those tribological properties was analyzed by measurements of Raman spectroscopy, observation of scanning electron microscope and non-contact type microscopy.

This study examined the tribological behavior of ta-C coating fabricated at a substrate bias of -100 V with FCVA deposition. Defect in ta-C coating was categorized with droplet, pore and spikes regarding with morphological, structural and mechanical properties of ta-C surface. Friction tests were conducted at a temperature

of 170 ℃ in ambient air using a ball on disk tribo-meter. Friction coefficient was 0.08 during a steady state and wear rate was 4.3×10^{-6} mm^3/Nm. To explain the friction and wear behavior, a shape and structural properties of defects in designated area was compared with a different sliding cycles. Droplets were remained during the friction test at 170 ℃ at designated area. During the sliding, formation of tribo-layer on Si_3N_4 ball prevented to form spike. These spikes became abrasive particles, resulting in severe wear at pore which had sp^2 rich structure and low mechanical properties.

Contents

List of Figures

List of Tables

Chapter 1 Introduction

1.1 Industrial needs of DLC coating

With the continuously increase of energy consuming, resource depletion and environmental pollution, importance of material and energy conservation is more and more emphasized. Definition of wear is removal or loss of materials occurring at the interface between sliding interface, which principally results in poor performance and material failure [1,2]. Friction is the force against the sliding motion of a body in opposite direction, which is the major factor of energy dissipation. It has been reported that one-third of the world's energy resource is due to overcome frictional loss in mechanical component [2,3]. Lubrication is a widely used means, which could effectively reduce wear and frictional loss.

Hence, tribology, defined as the science and technology of friction, lubrication and wear, is of great significance for the industrial growth and sustainability of development [4,5]. The study of tribology has been successfully applied to various application and attracted attention from numerous scientists in physics, chemistry, material science and mechanical engineering [3]. Some examples of tribological applications contain aircraft engines, automobile component, cutting tool and bio-medical application [6].

In the mechanical engineering field, automotive industry is the prime driving force behind the research of tribology, which is facing harsh international competition of technological innovation. Technological innovation requires enhancement of fuel efficiency and durability of mechanical components for modern cars. This concern is not only crucial to avoid major economic losses but also could relieve the environmental problem by reducing CO_2 emission. The most fundamental part of a car system is the internal combustion engine, and friction in the engine and power transmission system leads to about 17% of total energy losses in parts such as piston assembly or valve train [2]. Therefore, reducing the friction and wear in mechanical components of passenger cars could contribute the huge saving of energy, materials and maintenance cost.

It is noticed that the friction and wear are not material properties but two kinds of responses of a tribo-system, which are quite sensitive to condition parameters such as temperature, counterpart material or sliding speed [7]. Lubrication is essential for the machinery to increase the tribo-performance of sliding parts with friction reduction, wear protection and corrosion inhibition.

Generally, lubricants could be summarized into two types: solid lubricant and liquid lubricant. The current trend in modern tribology is to reduce the use of liquid lubricants as much as possible because of environmental concerns, but increase the

application of solid lubrication materials. Solid lubricants are able to self-lubricate the two surfaces sliding against each other without the need for a liquid oil medium such as graphite and molybdenum disulfide [8,9], and they could be applied to conditions of extreme contact pressure or high temperature. Solid lubricant coatings are primarily used to control friction and wear in high temperature environments, where conventional materials and lubricants cannot provide the desired levels of performance of durability [9–13]. During the past two decades or so, remarkable progress has been made in solid lubricant coating fields.

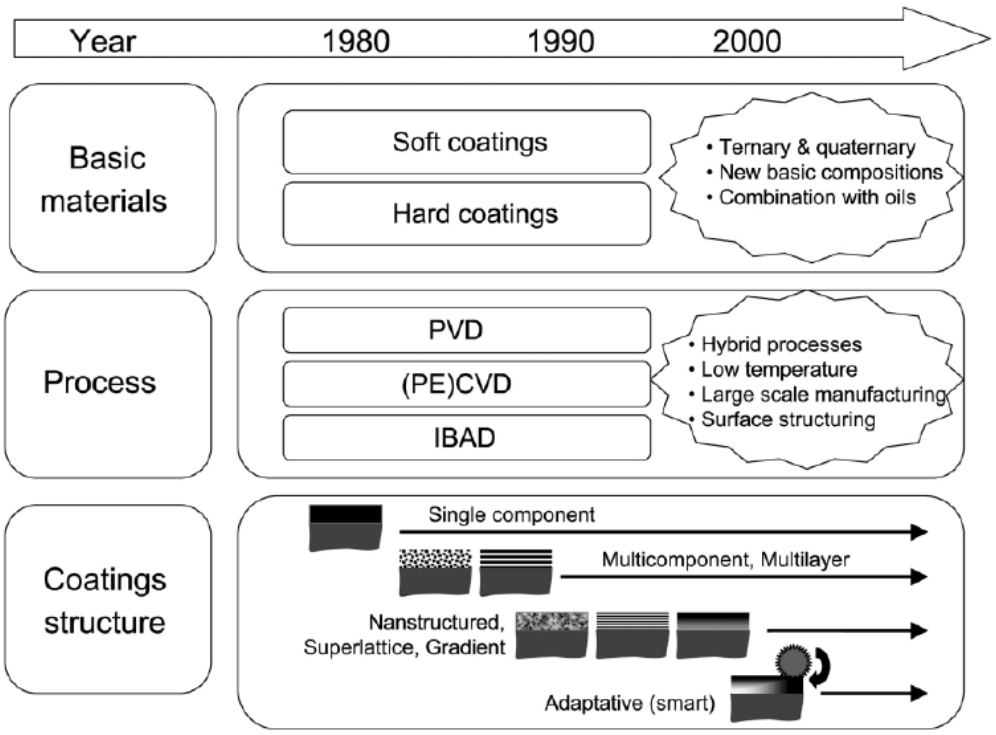

Figure 1.1 Historical developments of tribological coatings and solid lubricant films [9]

1.2 Carbonaceous hard coatings

1.2.1 Diamond-like carbon

Carbon is the 15th most abundant element in Earth and one of the key component outstanding elements. With different type of hybridizations like sp^3, sp^2 and sp^1 shown in Fig. 1.2, carbon could form single, double, and triple bonds [14]. Carbon is capable of forming multifarious allotropes, such as diamond, graphene, fullerene, carbon nanotube, etc. Among the carbon-based material, Diamond shows excellent properties such as superior mechanical properties and thermal conductivity. Graphite, another allotrope of carbon, exhibits high thermal conductivity and lubricating properties.

Over the past several decades, carbon has become the outstanding element for depositing thin coating like diamond, diamond-like carbon (DLC), and a numbers of metal carbide coatings [15,16]. In those carbonaceous materials, DLC coatings, dues to their superior mechanical and excellent tribological properties, are feasible for many application as shown in Fig. 1.3 [17,18]. The properties of various type of carbonaceous coating are compared in Table 1.1 [19].

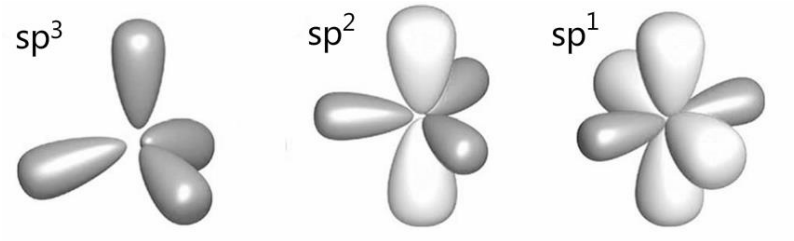

Figure 1.2 Different hybridizations for a carbon atom [14]

A variety of deposition methods have been introduced to deposit DLC coatings. Fabrication method of DLC coatings can be broadly categorized into two types: Physical Vapor Deposition (PVD) and Chemical Vapor Deposition (CVD). In PVD process, solid carbon source is evaporated and then adhere to substrate as a condensed phase, suitable for manufacture thin films requiring for mechanical, optical, chemical or electronic functions. PVD method is further divided into the arc, sputter, and laser vapor deposition methods [20–22]. While CVD method uses a gas (hydrocarbon such

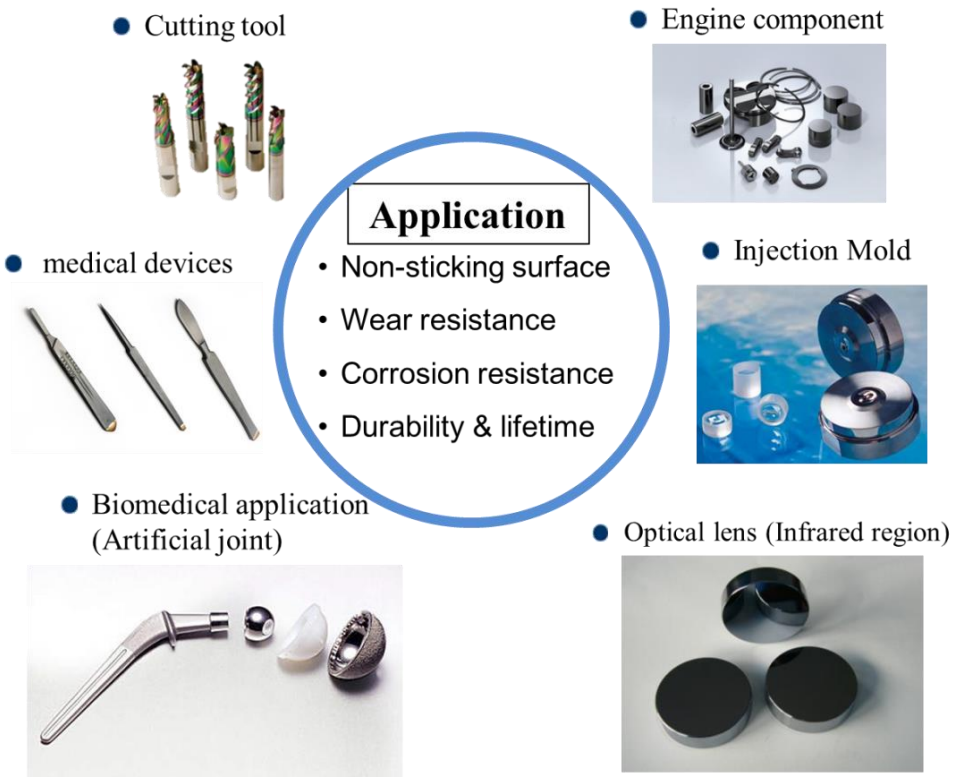

Figure 1.3 Various applications of DLC coatings: (a) cutting tool, (b) medical devise, (c) biomedical application, (d) engine component, (e) infection mold, and (f) Optical lens

Table 1.1. Property of various type of coating [19]

	Density (g/cm^3)	Hardness (GPa)	% sp^3	at. % H	Band gap (eV)
Diamond	3.515	100	100		5.5
Graphite	2.267		0		-0.04
C_{60}			0	0	3
Glassy C	1.3-1.55	2-3	~0		0.01
a-C, evap.	1.9-2.0	2-5	1		0.4-0.7
a-C, sputt.	1.9-2.4	11-15	2-5		0.4-0.7
a-C, MSIB	3.0	30-130	90±5	< 9	5.5-1.5
a-C:H, hard	1.6-2.2	10-25	30-60	10-40	0.8-1.7
a-C:H, soft	0.9-1.6	< 5	50-80	40-65	1.6-4
Polyethylene	0.92	0.01	100	67	6
ta-C	3.0	55-65	mainly	< 1	

as methane) as the carbon source for taking place a chemical reaction in the process with resulting in incorporation of hydrogen in its structure. Typical CVD method are metal organic chemical vapor deposition (MOCVD), Plasma-enhanced chemical vapor deposition (PECVD), radio-frequency (RF), direct current (DC) discharge, and self-discharge methods [23,24].

DLC coating has an amorphous structure with a mixture of the sp^3 structure (diamond) and the sp^2 structure (graphite), which makes it suitable tribological

candidate due to high hardness, low friction, and corrosion resistance. The structure of DLC coatings and the ternary phase diagram that describes structure depending on the sp^2, sp^3 bonding ratio and hydrogen concentration are represented in the Fig. 1.4, supposed by Ferrari and Robertson [25]. The properties of DLC coating on the ternary diagram greatly depend on sp^3/sp^2 ratio, in turn, it is directly affected by the deposition method and specific parameters, i.e. precursor, energy of particle and substrate bias [26,27].

DLC coatings are divided into hydrogenated amorphous carbon (a-C:H), hydrogenated tetrahedral amorphous carbon (ta-C:H), amorphous carbon (a-C) and non-hydrogenated tetrahedral amorphous carbon (ta-C). Hydrogenated DLC is relatively low friction coefficient but soft, meaning the poor wear resistance despite of thick coating with a good adhesion [28,29]. While non-hydrogenated DLC shows superior mechanical performance as a protective coating [30,31].

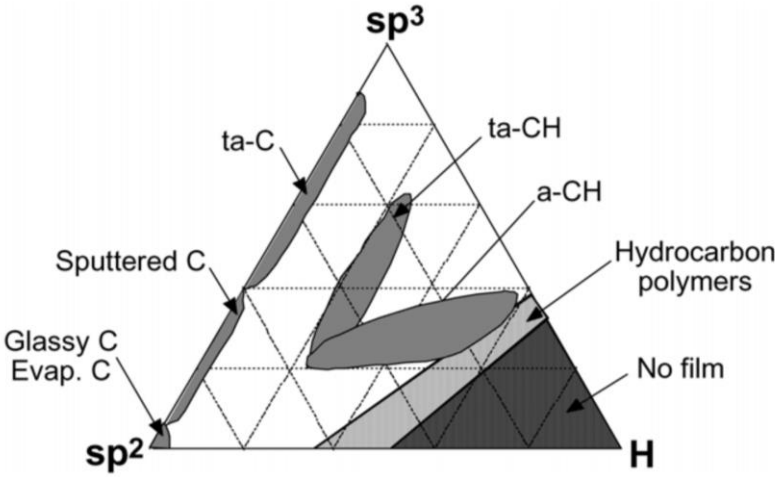

Figure 1.4 Structure and Ternary phase diagram of DLC coatings [32]

1.2.2 Tetrahedral amorphous carbon (ta-C) coating

Amorphous carbon coatings having high sp^3 bonded carbon content, referred as ta-C coating, occupies a special place because of higher hardness than other DLC coating. Over the years, The ta-C coating has attracted a great deal of attention from scholars in both experiment and production with providing superior tribological performance when used in magnetic hard disc applications [33–35].

The ta-C coating, have attracted considerable interest due to their unique mechanical, optical, structural and tribological properties. Among those properties, the mechanical properties of ta-C coatings made them attractive for wear resistance applications such as biomedical components, optical lens in infrared regions as transparent protective coatings and mechanical components.

Even though the ideal structure has not been synthesized until now, numbers of research groups have successfully fabricated ta-C coating via different deposition methods, such as magnetron sputtering [36–38], ion beam deposition [39], pulsed laser deposition (PLD) [40,41], and filtered cathodic vacuum arc (FCVA) [42–44]. Figure 1.5 shows the schematic illustration FCVA deposition system for depositing ta-C that includes argon ion gun for surface cleaning, and magnetron sputtering system for depositing inter-layer. FCVA system has been proven to be a reliable deposition technique for producing high quality ta-C coating. The detail of FCVA

system is mentioned below.

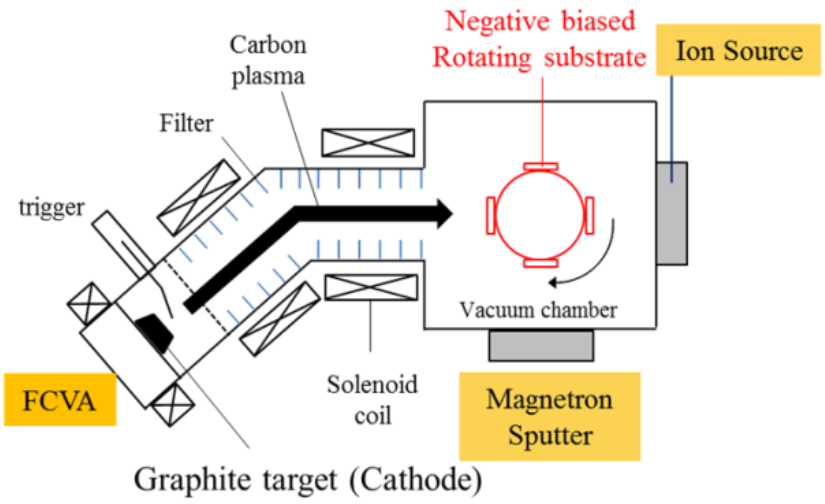

Figure 1.5 Schematic illustrations of methods used in deposition of ta-C coatings

1.3 Purpose of this dissertation

In 2nd chapter, the author tried to fabricate ta-C coatings with good stability and clarify their tribological properties at high temperature. At first, ta-C coating was fabricated by FCVA method for providing high density plasma and produce high quality of ta-C coatings. The mechanical and structural properties of the coating needed to be improved, because high hardness was coincided with the wear resistance, which may prevent delamination in high temperature condition. Thus, we controlled substrate bias of ta-C coating with a different substrate bias at 0, -100 and -300 V for changing its structural mechanical and tribological properties, and thus examined the thermal stability and tribological properties were clarified in high temperature

environments. Further details were described in part of 1.4.1 .

In 3rd chapter, it was found that formation of a transfer layer on counterpart material was important factor for running-in and wear behavior. The tribological properties of ta-C coating at high temperature compared to that under the room temperature showed longer running in cycle and poor wear resistance. To further improve thermal stability and wear properties, it is important to understand the relationship between tribological behaviour and growth of transfer layer on counter-part material in the view of surface morphology of ta-C coating because the tribological behaviour of ta-C coating depends on the surface roughness, defects like a pinhole and temperature. Further details were described in part of 1.4.2 .

Last in 4th chapter, the aim was to examine in detail the friction and wear behavior at high temperature in the view of morphology of ta-C coating deposited at a substrate bias of -100 V. Defects presented in ta-C coating surface were classified with their shape, structural and mechanical properties. The role of defects on tribological behavior was revealed by comparing the change of structural, mechanical and morphological properties. Further details were described in part of 1.4.3 .

The purpose of this dissertation is summarized with the followings:

1. To clarify the effect of substrate bias on structural properties and tribological behavior of ta-C coating (Chapter.2).

2. To clarify the effect of temperature on structural properties and tribological behavior of ta-C coating (Chapter.2).
3. To reveal origin of the running-in cycle in the view of morphology presented on ta-C coating surface and observe formation of transfer layer with a different sliding cycles (Chapter.3).
4. To classify the type of defects in ta-C coating and clarify the effect of each defects on tribological properties of ta-C coating (Chapter.4).

1.4 ta-C coating deposited with FCVA system

1.4.1 Substrate bias

In the previous research, the effect of sp^2 and sp^3 content on the mechanical and structural properties of DLC coating has been investigated [45,46]. For ta-C coatings, various studies have reported from the microstructural and mechanical properties perspective [47–49] that the properties of the coating is greatly dependent on the bias voltage and other deposition parameter such as arc current and duct bias [50–52]. Increasing a substrate bias up to -100 V, the carbon network could remain predominantly tetrahedral, whereas further increase of bias voltages favors an increase of sp^2 bonding. Substrate bias is found to be an effective way to adjust the

sp^3 and sp^2 ratio in the coating. The relationship between sp^3 ratio and I_D/I_G confirmed with XPS and Raman analysis are to be seen in Fig. 1.6. By controlling the substrate bias might gain benefits in terms of superior structural and mechanical properties at a substrate bias of -100 V as shown in Fig. 1.7.

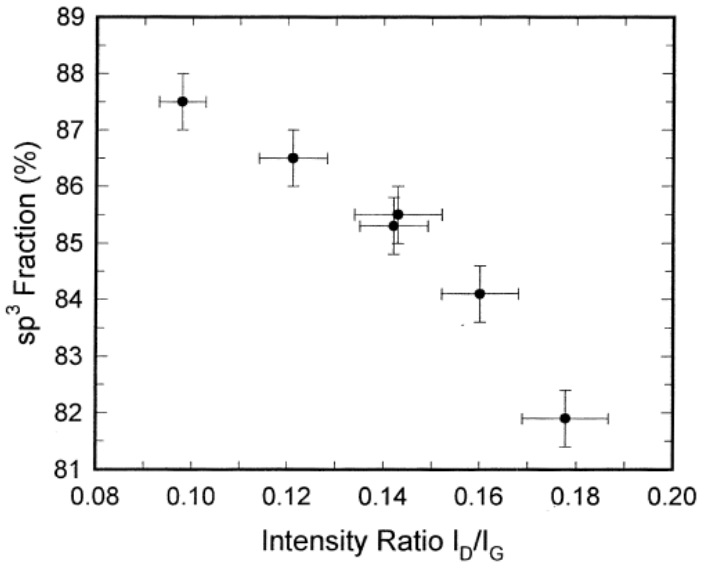

Figure 1.6 sp^3 fraction as a function of intensity ratio I_D/I_G [57]

Ta-C coating could have better mechanical properties than amorphous carbon, and also overcome the limit of ta-C coating in high temperature condition, making ta-C with great potential for the mechanical and tribological application of actual industry [53–56]. From the review mentioned above, studies of ta-C so far are mainly about the depositing parameters and material properties, and there are few about the tribological properties of ta-C coatings. With the increase of substrate bias, the structure and mechanical properties of the coating is reported to change. Since the

structure and mechanical properties of these coatings is crucial for the tribologcial application, in this study to fabricate ta-C coating more suitable for mechanical sliding parts, carbon is ionized by cathodic arc, controlling the substrate bias of substrate.

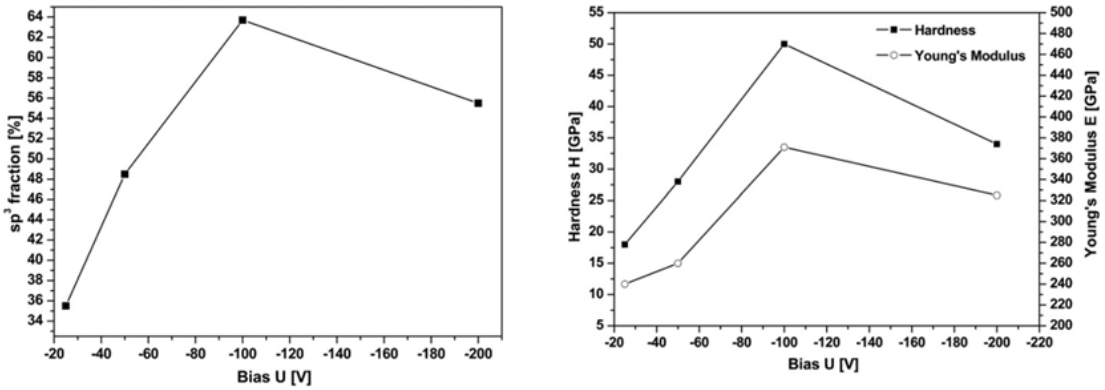

Figure 1.7 sp^3 content and Hardness and Young's modulus of ta-C coatings deposited by FCVA [58]

In the past two decades, ta-C coatings have been studied extensively. For example, the some authors focus on the fabrication and structure of ta-C by using different deposition system. The tribological properties of ta-C coating also have been investigated, such as the effect of counter-part material, effect of substrate bias and effect of doping element [46,59–61] and high temperature conditions as shown in Fig. 1.8. Although many researchers have made considerable effort on the ta-C coatings, the tribological behaviors and tribological mechanism at high temperature are still not clarified yet.

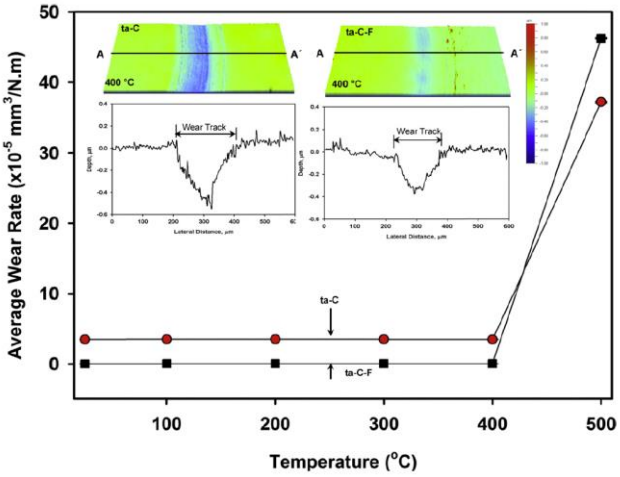

Figure 1.8 Average wear rate as a function of testing temperature in ta-C coatings [56]

1.4.2 Formation of transfer layer and defects of ta-C coating

FCVA system has been proven to be a reliable deposition technique that can produce high sp^3 bonding ta-C coating. The principal problem related to the vacuum arc deposition is the micro-particles and defects presented on ta-C coating surface [62–65].

In this regard, it is important to understand micro structure of ta-C coating which is relationship between coating durability and performance of application. In additionally, the durability of ta-C coating depends on the surface roughness, defects like a pinhole and temperature.

In previous research, many studies have been carried out to reveal the relationship between DLC coatings and wear properties. Y. Mabuchi et al. [66] reported the effect of the dropping out of droplets on ta-C coating fabricated by FCVA method under a

lubricated condition. D. Drescher et al. [67] showed the morphology and structural properties of DLC films deposited by Laser arc arrangement. H. Takikawa et al. [62] analyzed the droplets generated during the deposition process using T-FAD system and suggest the minimization method of droplets. A. Dorner et al. [68] deposited DLC coating with a different thickness and characterized the structural and durability of DLC coating as a function of coating thickness.

However, there are few investigations for effect morphology and defects in ta-C coating on wear and friction behavior. Therefore, the purpose of this study is to investigate the influence of defect and transfer layer on the friction and wear behavior which is able to help in understanding running-in cycles at high temperature condition. The main attention is paid to the mechanism of transfer layer and wear behaviour.

1.4.3 FCVA system

The deposition method is supposed to be dealt because type and properties of DLC is directly affected by the deposition method and specific parameters. Among the various kinds of deposition methods in PVD, the sputtering deposition (sputt.) and electron beam evaporation (evap.) in which carbon is deposited on to the substrate without ionization process, have a disadvantage of low deposition rate [69]. Ta-C coatings were deposited by using a wide variety of deposition method including mass

selected ion beam (MSIB) [70], sputtering [71], pulsed laser ablation [72,73] and FCVA [20,21,74] with a high deposition rate.

Among other PVD methods for the preparation of ta-C coating, the cathodic arc deposition technique is particularly useful as it could provide highly ionized plasma of energetic carbon ions [75]. At the cathode spot region, very dense plasma is generated, and the evaporated cathode material (usually graphite) is ionized and the ions deposit solid hard coating on the substrate. The cathodic vacuum arc is a relatively low voltage process with high current density of discharge. However, the principal problem involved in this deposition method is the micro-droplet that is co-emitted from the cathode spot.

These micro-droplets adhere to the coating in preparation and roughen its surface, causing deterioration in the composition uniformity and exfoliation of the film. The incorporation of these macro particles in the film not only causes morphological imperfections but also degrade the tribological, electronic and optical properties.

To overcome the droplet problem, recent filtered systems designed particularly for preparing hydrogen-free ta-C coating are introduced [62]. The variety of different filtering techniques has been presented in Fig. 1.9. FCVA system has been designed particularly for ta-C preparation using graphite cathode with the idea that the transportation direction of plasma and the trajectory of droplets are separate from each

other, using the mechanical filter duct [21,50,76]. The function of the filter called to baffles is to prevent the multiple scattering sub-micron particles into the sample. However, it is hard to prevent to the inflow of particles generated from the edges of the baffles. Also the degree of duct can limit the plasma transport efficiency of the duct [64,77,78].

For the preparation of ta-C coatings, the FCVA technique with a duct of 45^{o} degree was particularly useful for industrial applications because it provided highly ionized plasma of energetic carbon ions, from which dense films of amorphous carbon could be grown onto large areas with relatively high deposition rates [79–81]. Therefore, in our group to ta-C coating, FCVA system with a duct of 45^{o} degree has been selected instead of the other method that is ta-C deposition with its different electromagnetic plasma transportation duct or droplet filter configurations.

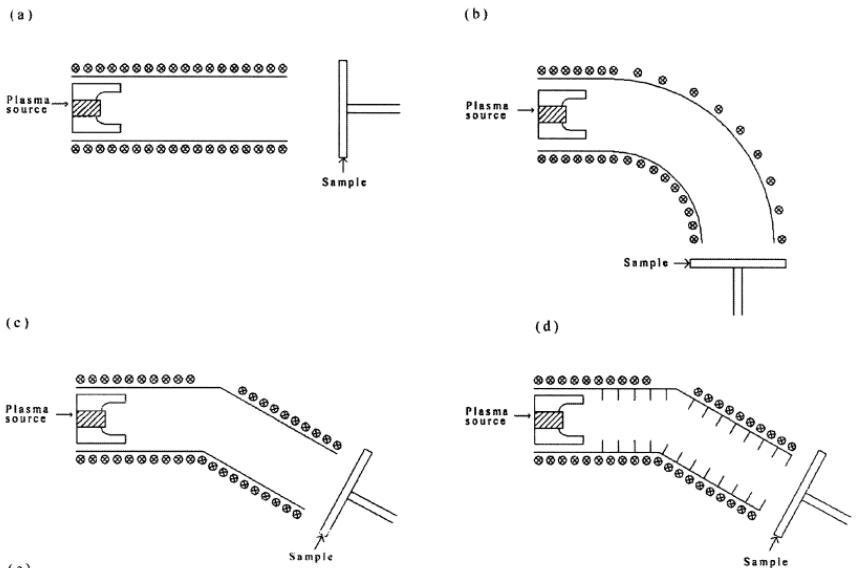

Figure 1.9 Schematic sketches of the magnetic filtering designs. (a) Straight duct; (b) toroidal duct; (c) knee duct; and (d) knee duct with baffles [21]

1.5 Outline of this dissertation

This dissertation presents the tribological behaviors of ta-C coatings in high temperature condition. This first chapter introduces an overview of ta-C coatings and their deposition method, as well as the purpose of this study. Chapter 2 presents outcomes of our investigations on relations between substrate bias and tribological behaviors in elevated temperature. Chapter 3 reveals factor for running-in cycles and the relationship between transfer layer and wear behavior. Chapter 4 presents outcomes of our investigations on the effect various type of defects in ta-C coating surface on tribological behaviors. At last, Chapter 5 presents a summary of all findings of this dissertation. Figure 1.10 presents graphically the organization of the dissertation

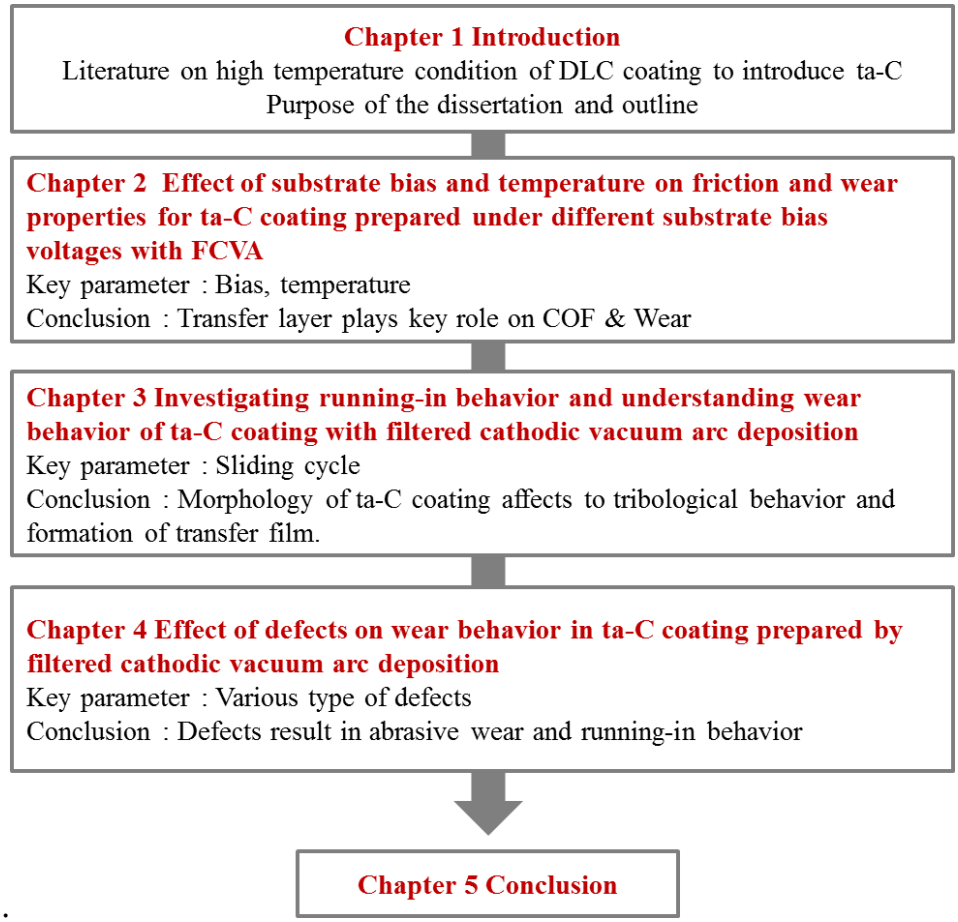

Figure 1.10 Organization of this dissertation

Chapter 2
Effect of substrate bias and temperature on friction and wear properties for ta-C coating prepared by filtered cathodic vacuum arc deposition

2.1 Introduction

Diamond-Like Carbon (DLC) coatings consisted of sp^2 and sp^3 bonded carbon atoms have received considerable attention because of their attractive properties like a high hardness, high resistivity and low friction coefficient [60,82,83]. These properties make them useful for many industrial applications such as wear resistance and protective coatings for cutting tools, biomedical application and engine components. However, those operations are performed at high temperatures and generating frictional heat during contact, these makes tribological properties of DLC coatings deteriorate rapidly [84–87].

These DLC coatings can be classified into hydrogen-free tetrahedral amorphous carbon (ta-C), hydrogen-free amorphous carbon (a-C), hydrogenated ta-C (ta-C:H), and hydrogenated a-C (a-C:H) depending on the sp^2/sp^3 ratio and hydrogen content.

Among the type of DLC coatings, non-hydrogenated tetrahedral amorphous carbon (ta-C) is an ideal candidate for those application due to good thermal stability attributed to high sp^3 content, which contain more than 80 %. Various methods have been employed for depositing ta-C coatings, such as plasma-enhanced chemical vapor deposition (PE-CVD), Filtered cathodic vacuum arc (FCVA) and sputtering deposition [51,80,88]. Among these methods, FCVA deposition is a suitable technique for the mass production of high quality ta-C coating. It has been reported by many researchers that high sp^3 ratio was obtained by controlling the substrate bias [62,66,68,89]. However, it is not clear how ta-C coating containing higher sp^3 ratio enhance the wear resistance at elevated temperature.

This chapter focused on ta-C coatings fabricated at different substrate bias potential at 0, 100 and 300 V sliding against a silicon nitride (Si_3N_4) ball by conducting ball-on-disk tests at elevated temperatures up to 600 ℃ to characterize the relationship between physical properties and tribological behavior.

2.2 Experimental

2.2.1 Coating deposition

The ta-C coatings investigated in this study were deposited on Inconel disks with dimension of 20 mm in diameter and 2 mm in thickness and P-type Si wafers with

size of 40×10×0.3 mm^3 by using a FCVA system illustrated in Fig. 2.1. A 45° curved filter was employed to remove all unwanted neutral atoms and macro-particles (Fig. 2.2). A substrate holder was rotated at a constant speed for uniformity with the exit of FCVA source to substrate of 15 cm. Prior to the deposition, the substrate was thoroughly cleaned ultrasonically in alcohol and de-ionized water. The deposition base pressure was below 5×10^{-3} Pa. Before deposition, argon ion beam bombardment was employed to remove the oxide layer and impurities on surface of the silicon and Inconel disk composed with nickel (68 %), chrome (17 %) and iron (8 %). An Inconel disk was well suited for this study requiring high strength and good corrosion resistance in high temperature due to investigating tribological behavior of top surface of ta-C coating. A chromium layer was deposited to enhance the adhesion between the substrate and ta-C coatings. The deposition was carried out at an applied an arc current of 60 A. Three set of samples was deposited using a different negative substrate bias voltage of 0 V (0 V ta-C coating), 100 V (100 V ta-C coating) and 300 V (300 V ta-C coating) in Fig. 2.3. The detailed deposition condition of ta-C coating was described in Table 2.1.

Table 2.1. Deposition condition of ta-C coatings with ion beam cleaning and sputtering system

ION Beam	Rotate (rpm)	Gas (Ar)	Bias (-V)	PID Power (V/mA)	Time (min)		
	10	16	0	1700/150	50		
ION Beam+Sputter	Rotate (rpm)	Gas (Ar)	Bias (-V)	PID Power (V/mA)	UBM Power (W)	Time (min)	
	10	200	0	1700/150	400	2	
Sputter (Cr)	Rotate (rpm)	Gas (Ar)	Bias (-V)	UBM Power (W)	Time (min)		
	10	200	0	400	17		
Pre-coating	Rotate (rpm)	Gas (Ar)	Bias (-V)	Arc Power (A)	Duct Power (V)	Magnet system	Time (min)
	10	2	600-350	60	10	Y	3+3
Main-coating	Rotate (rpm)	Gas (Ar)	Bias (-V)	Arc Power (A)	Duct Power (V)	Magnet system	Time (min)
	10	2	100	60	10	Y	64

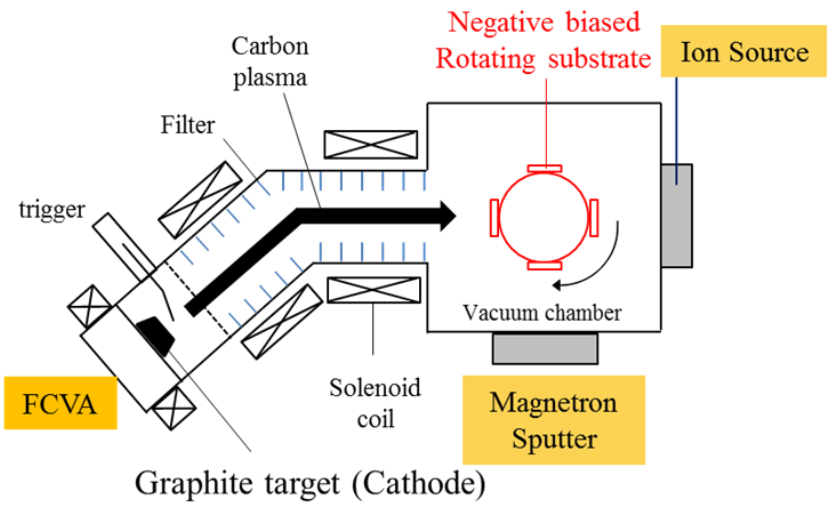

Figure 2.1 Schematic diagram of the FCVA system

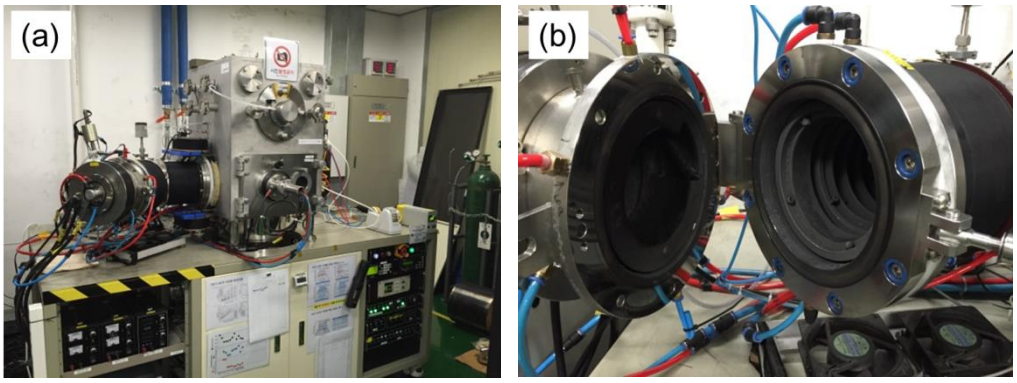

Figure 2.2 Photographs of (a) FCVA system and (b) Arc cathode and baffle duct

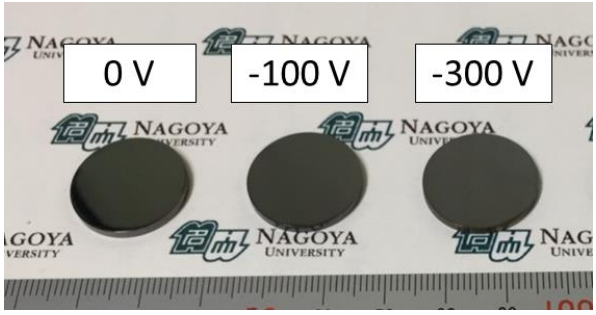

Figure 2.3 ta-C coatings deposited at different substrate bias at 0, -100 and -300 V

2.2.2 Tribological experiments

The tribological performance of ta-C coatings in Inconel disk was confirmed by using a high-temperature ball-on-disk type tribo-tester to evaluate the friction, as illustrated in Fig. 2.4. These specimens were preheated to 23, 100, 200, 300, 400, 500 and 600 ℃, respectively in ambient air via an Infrared lamp and temperature was maintained at the set value during the friction test. A silicon nitride (Si_3N_4) ball (Φ=8 mm) was used as a counter part material with the wear track radius of 3 mm. For each test, a load of 1 N was applied on a Si_3N_4 ball rotating at a sliding speed of 200 rpm until completion of 10000 revolutions.

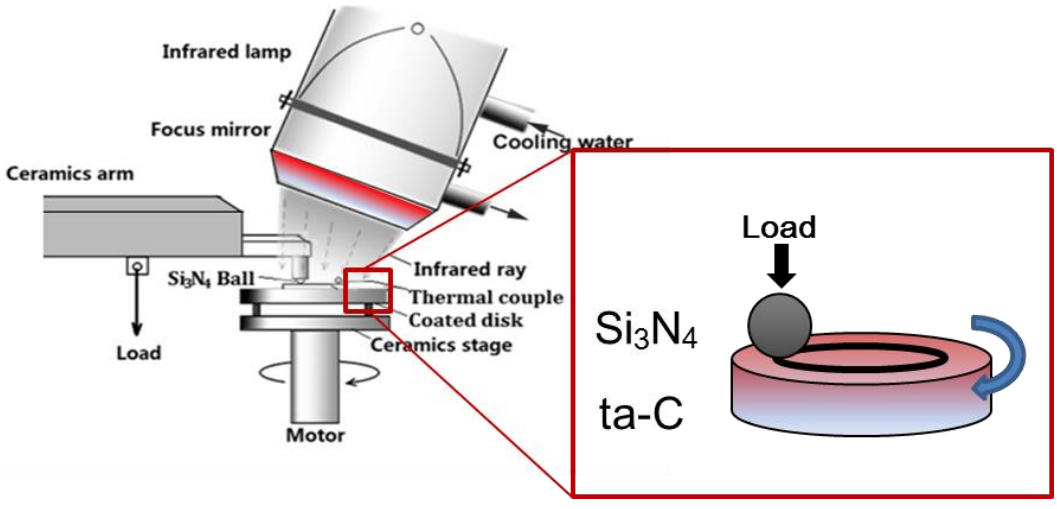

Figure 2.4 Schematic of ball-on-disk tribo-tester

2.2.3 Coating characterization and surface analysis

The microstructure of the wear tracks and wear scars on the coating and ball were measured by using Raman spectroscopy (Jasco, NRS-1000), with 532 nm laser in the wave ranges of 600-2200 cm^{-1} and examined by optical microscopy as illustrate in Fig. 2.5. The hardness of the ta-C coatings was characterized by a nano-indentation tester with a Berkovich indenter under applying load of 1000 μN (Elionix, ENT-1100a,). The curvature of the ta-C coatings were measured by using a Residual stress tester (J&L tech, Residual Stress Tester) and the residual stress of the ta-C coating were calculated using Stoney's equation. Nano-indentation tests and Residual stress tests were conducted 10 times and the average values were obtained. The thickness of the coatings was measured by a surface profiler (Mitsutoyo, S-3000). I_D/I_G ratio and G peak position was calculated to study the effect of substrate bias and temperature on the structural evolution of the coatings and formation of transfer layer. Table 2.2 shows the characteristic parameters of ta-C coatings. The wear rates of ta-C coating were calculated by cross-sectional of wear tracks measured by a Non-contact surface profiler (ZYGO, Newview6200) at four different measurement point. Wear track on the coatings were observed by the ZYGO to quantify the specific wear rates, calculated by using the wear equation where V is the wear volume (mm^3), W is the load (N), and L is the sliding distance (m). For the calculation of residual stress (σ_f) of ta-C coatings,

$E_s/(1-v_s)$ present elastic constant equivalent to 180, h_s is thickness of substrate, k is curvature and h_f is thickness of ta-C coating.

$$\text{specific wear rate} = \frac{V}{W \times L} \quad , \tag{2.1}$$

$$\text{Residual stress } (\sigma_f) = \frac{E_s \times h_s^2 \times \mathrm{k}}{6h_f(1-v_s)} \quad , \tag{2.2}$$

The morphology and roughness of the coatings and counterparts before and after the friction were measured by atomic force microscopy (AFM; Nanopics 1000, SEIKO). The measurement of roughness Ra of wear scar of coating was from the square of side length of 150 μm containing wear scar inside, and the roughness Ra of the wear track of counterpart was evaluated from the four cross-symmetrical squares of side length of 20 μm inside the circulate wear track.

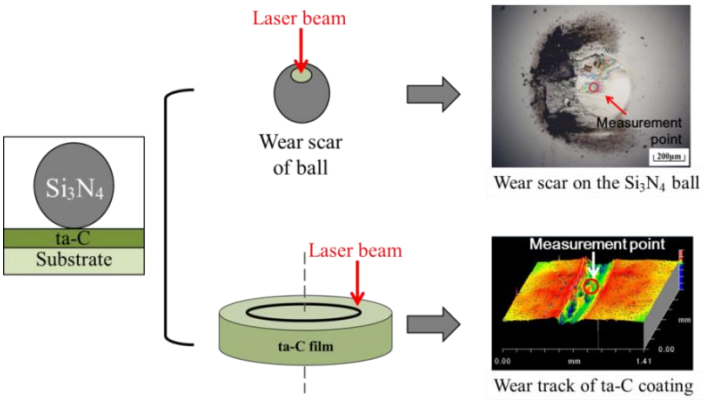

Figure 2.5 Measurement point for Raman analysis of wear scar on the Si_3N_4 ball and wear track of ta-C coating

2.3 Results and Discussion

2.3.1 Effect of substrate bias on structural and mechanical properties

The Raman spectra of ta-C coatings deposited with different substrate bias of 0, -100 and -300 V were measured. The Raman spectrum can be deconvoluted into two bands of ta-C coating. Figure 2.6 shows intensity ratio of the D-band to the G-band (I_D/I_G) characteristic as a function of the substrate bias. The I_D/I_G ratio decreased with the substrate increased to substrate of -100 V. Further increasing substrate bias of -300 V, I_D/I_G ratio slightly increased.

Ferrari and Robertson suggested a qualitative interpretation method for structure of ta-C coating from the I_D/I_G ratio [90]. Figure 2.6 showed that the lowest I_D/I_G ratio was attained in ta-C coatings fabricated at negative substrate bias of 100 V. This result means that 100 V ta-C coating have a higher sp^3 content compared to the other coatings deposited at other substrate bias voltage. In additional, a value of substrate bias may have a strong influence on physical and mechanical properties of the ta-C coatings. The increase of the bias voltage from 0 to 100 V improves the hardness of the deposited ta-C coatings from 29.4 GPa to 35.2 GPa. As the substrate bias increases more than 300 V, mechanical properties seemed to be saturated. The maximum hardness was obtained at the bias voltage of 100 V. These results are in agreement with the results of sp^3 content

estimated from I_D/I_G ratio and residual stress as shown in Table 2.2.

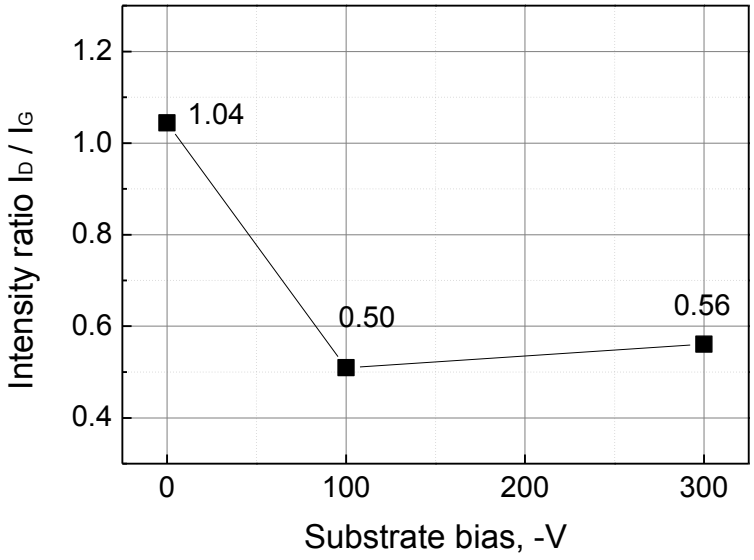

Figure 2.6 I_D/I_G ratio of ta-C coating on Inconel disk as a function of negative substrate bias

Table 2.2. Coating characteristics of various nitrogen content ta-C coatings

Samples	Applied substrate bias, -V	Thickness, nm	Hardness, GPa	Residual stress, GPa	Roughness, nm	I_D/I_G	G peak Position, cm^{-1}
0V ta-C	0	1142	29.4	2.23	376	1.04	1555.9
100V ta-C	100	1085	35.2	4.05	434	0.50	1563.7
300V ta-C	300	1047	35.0	3.70	259	0.56	1375.2

2.3.2 Tribological performance

Figure 2.7 (a) presents the friction coefficient (μ) of ta-C coating fabricated at substrate bias of 0 V versus sliding cycles tested at different temperatures. Average

steady state in friction coefficient was defined as the region after the running-in cycles referred to fluctuation of friction coefficient in an initial term. At room temperature, the steady state friction coefficient was 0.07, slightly higher than what exhibited at high temperature over 100 ℃. When tested at 100, 200, 300, 400 and 500 ℃, the average friction coefficient generated lower friction coefficient below 0.03. Meanwhile, at 600 ℃, the average friction coefficient of the ta-C coatings decreased, reaching 0.02 after running-in cycles, then increases abruptly at 4000 cycles, at which point the test was stopped.

Figure 2.7 (b), (c) present the friction coefficient values of ta-C coating deposited at substrate bias of 100 V and 300 V with a number of cycles at different testing temperatures. At 23 ℃, the steady state friction coefficient was 0.04, slightly higher than what overserved at higher temperature but stable state was maintained both of 100 V and 300 V ta-C coating. At 100 ℃, longer running-in cycles start to be seen at around 7000 cycle for 100 V ta-C coating and 4000 cycle for 300 V ta-C coating. More than those sliding cycles steady state was shown. After 200 ℃, these running-in cycles was decreased. Figure 2.8. showed a summary of the running-in cycles of the ta-C coatings with different testing temperature from 23 to 500 ℃. Highest running-in cycles was shown at 100 ℃ both of 100 V ta-C and 300 V ta-C coating and further increasing temperature up to 500 ℃, running-in cycles was decreased.

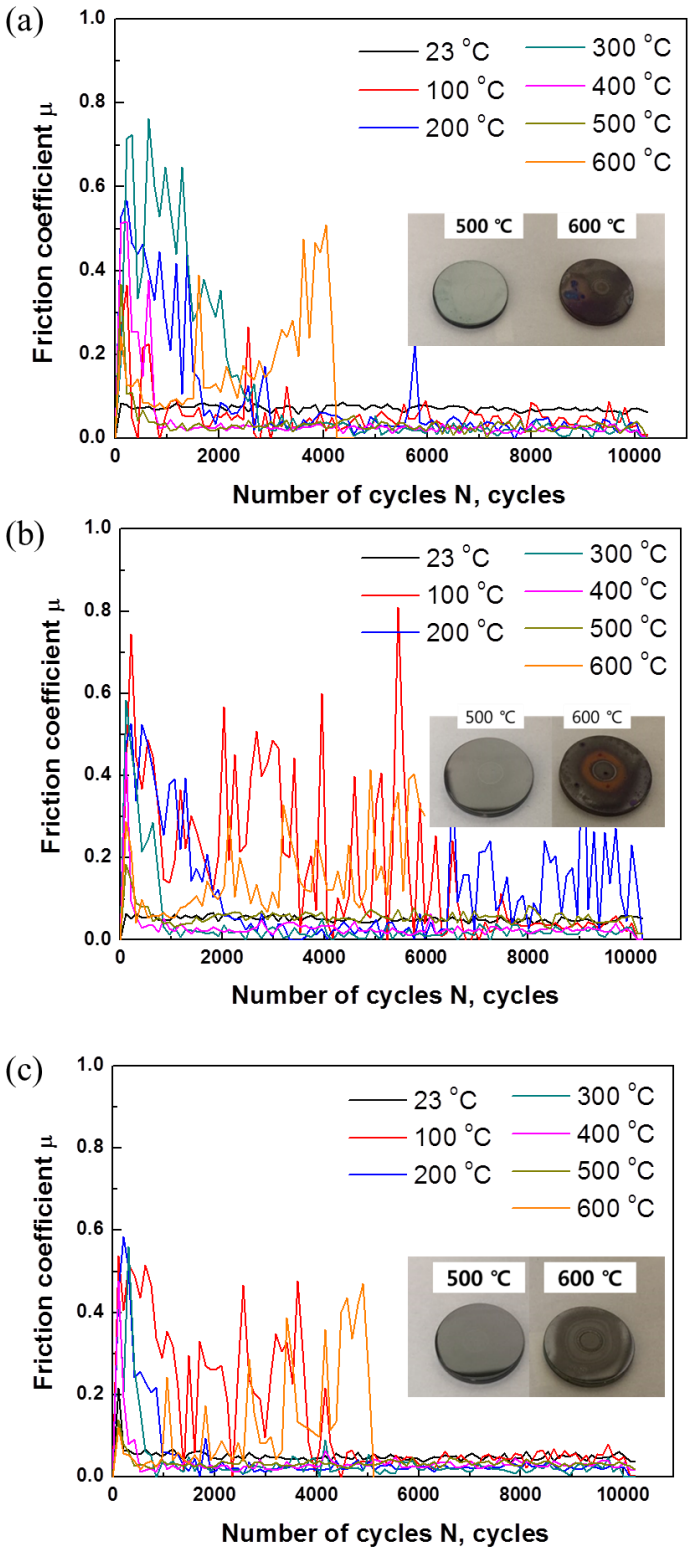

Figure 2.7. Friction coefficient of ta-C coatings fabricated by different substrate bias at (a) 0 V, (b) -100 V and (c)-300 V as a function of the number of sliding cycles at elevated temperature

Tribological behavior of the 0 V ta-C coating was studied with that of the 100 V ta-C and 300 V ta-C coating against Si_3N_4 ball. Figure 2.9 (a) shows the specific wear rate of 0 V ta-C coating as a function of testing temperatures. At 23 ℃, the track presented lower wear rate of 4.95×10^{-7} mm^3/Nm, compared by higher temperatures (>100 ℃). At 100 ℃ and 200 ℃, wear rate values of 4.45×10^{-6} mm^3/Nm and 4.72 $x10^{-6}$ mm^3/Nm were obtained respectively. With increase of temperature up to 300 ℃, further increase of wear rate of ta-C coating more was shown, reaching 6.57×10^{-6} mm^3/Nm. When tested at 400, 500 ℃, the wear rate remained a value in the range of 5.57×10^{-6} mm^3/Nm.

In the case of the 100 and 300 V ta-C coating illustrated in Fig. 2.9 (b) clearly characterized the different wear behavior compared to the 0 V ta-C coatings. In the case of 100 V ta-C, the lowest wear rate 9.65×10^{-7} mm^3/Nm was obtained at 23 ℃. At 100 ℃, sharply increase of wear rate is observed and reaches values of 9.22×10^{-6} mm^3/Nm. Above the temperature of 200 ℃, the wear rate decreased, recording 1.92×10^{-6} mm^3/Nm at 500 ℃. For 300 V ta-C, overall trend of specific wear were very similar and lower to those observed at 100 V ta-C. At 23 ℃, the specific wear rate was 5.25×10^{-7} mm^3/Nm. However, at 100 ℃, the specific wear rate increased by an order of magnitude to 7.32×10^{-6} mm^3/Nm. Further decreases in wear rate wear recorded from 200 ℃ (3.65×10^{-6} mm^3/Nm) to 500 ℃ (1.32×10^{-6} mm^3/Nm). Those

specific wear rates of 0 V, 100 V and 300 V ta-C coating was summarized in Table 2.3.

After the friction tests, the wear scar was apparent in the contact area. In order to explain the difference in friction coefficient and wear behavior after increasing the testing temperature, the wear scars on the Si_3N_4 ball were studied by using optical microscopy, as illustrated in Fig. 2.10. On wear scar of Si_3N_4 balls against 0, 100 and 300 V ta-C coating at temperature of 23 ℃, there were a few powder-like wear debris particles around the contact area. Even more explicit demarcation of the contact area damaged by ta-C coating can be seen. In the contact area, there were blue parts, discussed in more detail later. The structure of these blue parts was characterized by Raman analysis. At 100 ℃, a black powder like particles were observed around the wear scar, evidently showing that transfer layer started to be form on the Si_3N_4 ball. In additionally, after increasing temperature up to 500 ℃, wear debris transferred from the ta-C coating, covering the wear scar on the Si_3N_4 ball. The diameter of wear scar increased from 23 ℃ to 100 ℃ and then decreased with that from 100 to 500 ℃ both for 0 V ta-C, 100 V ta-C and 300 V ta-C coating.

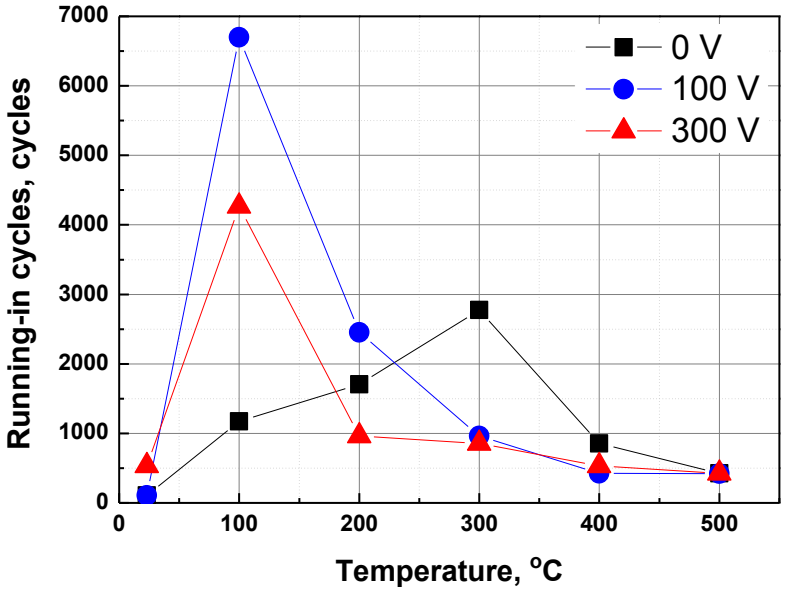

Figure 2.8. Variation of running-in cycles of the friction coefficient in ta-C coating fabricated by different substrate bias with a testing temperature from 23, 100, 200, 300, 400 and 500 ℃.

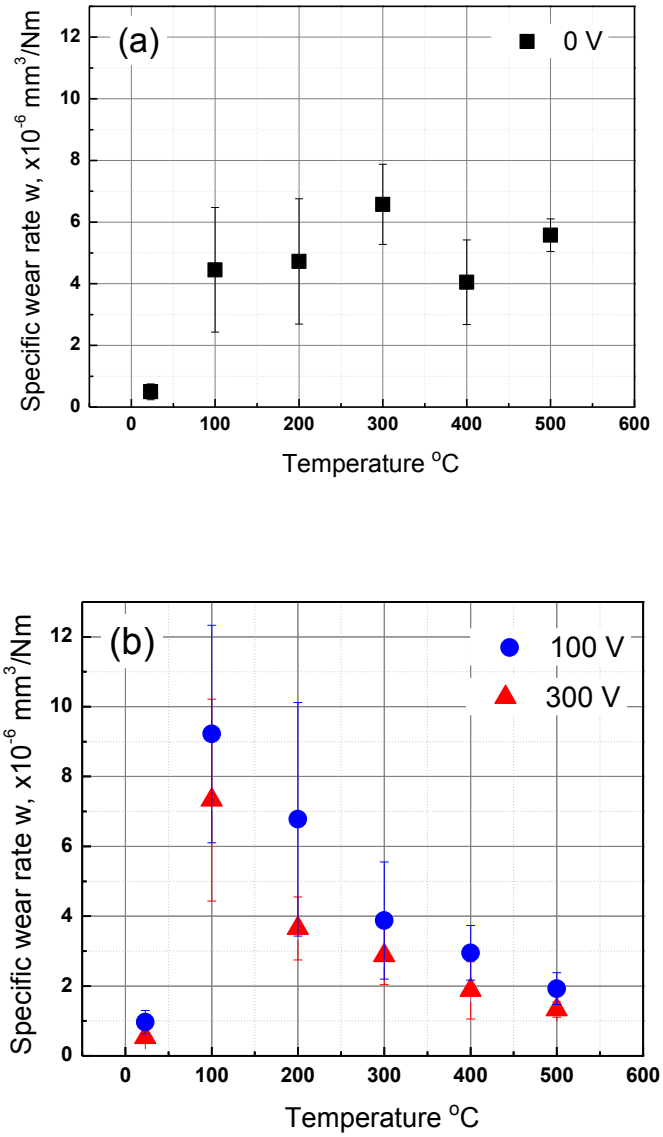

Figure 2.9. The variation of the wear rate of (a) 0 V, (b) 100 V and 300 V ta-C coatings with different testing temperature.

Table 2.3. Specific wear rate of ta-C coating as function of testing temperature (×10^{-6} mm^3 /Nm)

Temperature / Sample	23 ℃	100 ℃	200 ℃	300 ℃	400 ℃	500 ℃
0 V	0.49	4.45	4.72	6.57	4.05	5.57
-100 V	0.95	9.25	6.77	3.87	2.95	1.92
-300 V	0.52	7.32	3.65	2.87	1.87	1.32

2.3.3 Structural change and presence of carbonaceous transferred layer

In order to examine the formation of a carbon transfer layer, wear scars on the ball were investigated by Raman spectroscopy. Figure 2.11 (a), (b) and (c) presents the Raman spectrum from the center of each wear scar against 0 V ta-C coating, 100 V ta-C coating and 300 V ta-C coating. These results show a characterization of a transfer layers forming on the wear scars occurred at 100, 300 and 500 ℃. On the contrary, only Si_3N_4 peak was observed on the wear scar for 23 ℃. Therefore, these results mean that a carbon transfer layer was developed on the ball scar surfaces over 100 ℃, whereas there is no formation of such a transfer layer at 23 ℃.

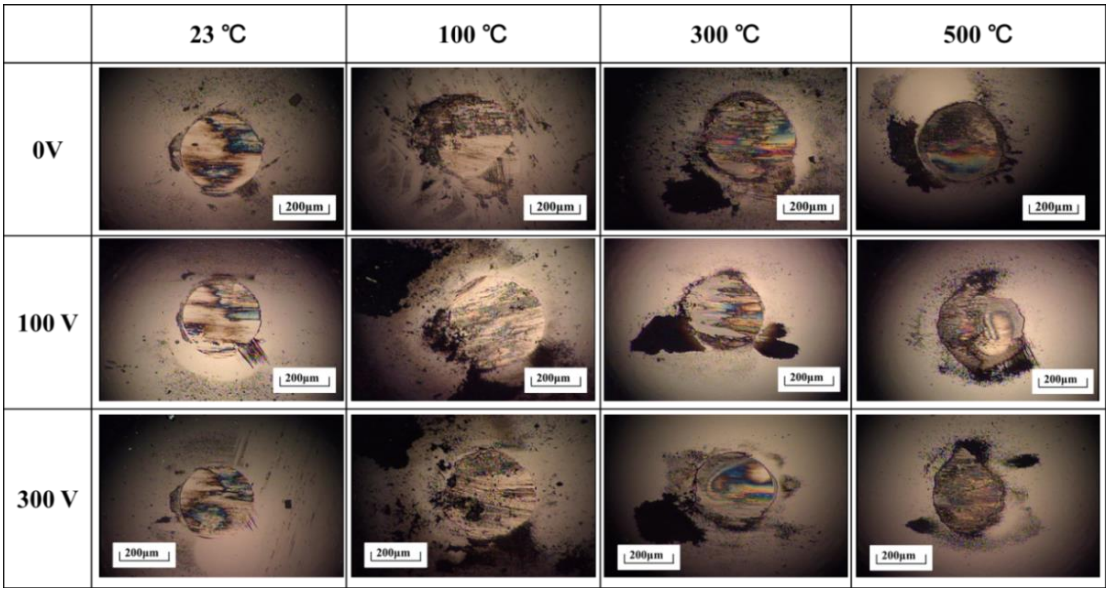

Figure 2.10. Optical microscope images of (a) the wear scar on the Si_3N_4 ball and (b) wear track on the ta-C coatings tested at different temperature.

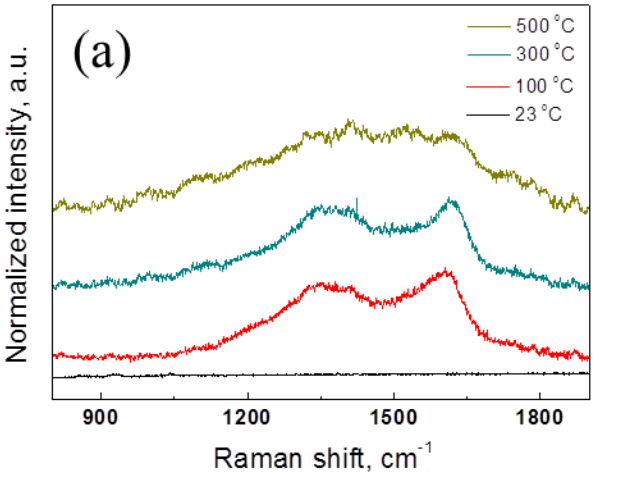

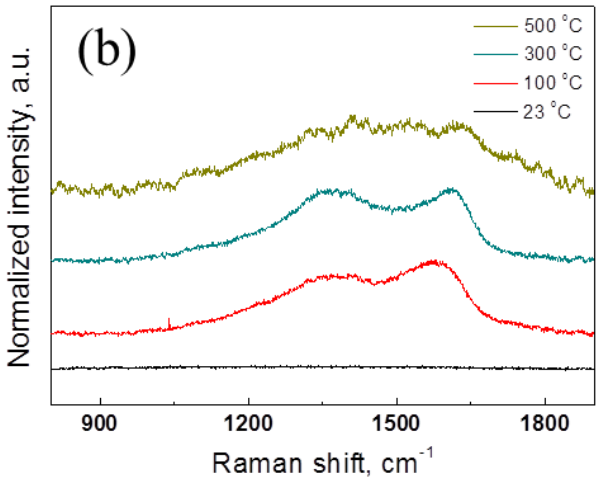

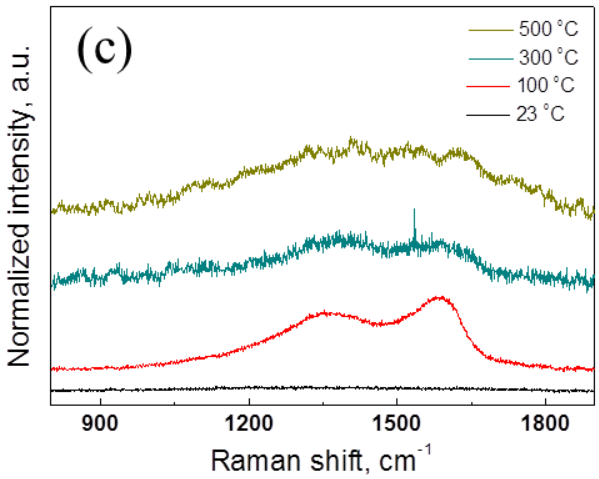

Figure 2.11. Raman spectrum, as measured at the center of the wear scar of Si_3N_4 ball versus (a)0 V ta-C coating, (b) 100 V ta-C coating and (c) 300 V ta-C coating.

To confirm structural evolution of ta-C coating as function of testing temperature, the structure of the coatings was also examined by Raman spectroscopy. Figure 2.12 showed Raman spectrum measured on the inside of wear track of 0 V ta-C coating, 100 V ta-C coating and 300 V ta-C coating. All Raman spectra were deconvoluted into D and G peaks and then calculated to determine I_D/I_G ratio. There was an increase in the I_D/I_G ratio of 0 V, 100 and 300 V ta-C coating after increasing the temperature. These results suggest that graphitization was taking place, as evidenced by increase of I_D/I_G ratio at elevated temperature. Tendency of graphitization of 0 V ta-C coating estimated from the slope of the plot was higher than 100 V and 300 V ta-C coating at elevated temperature.

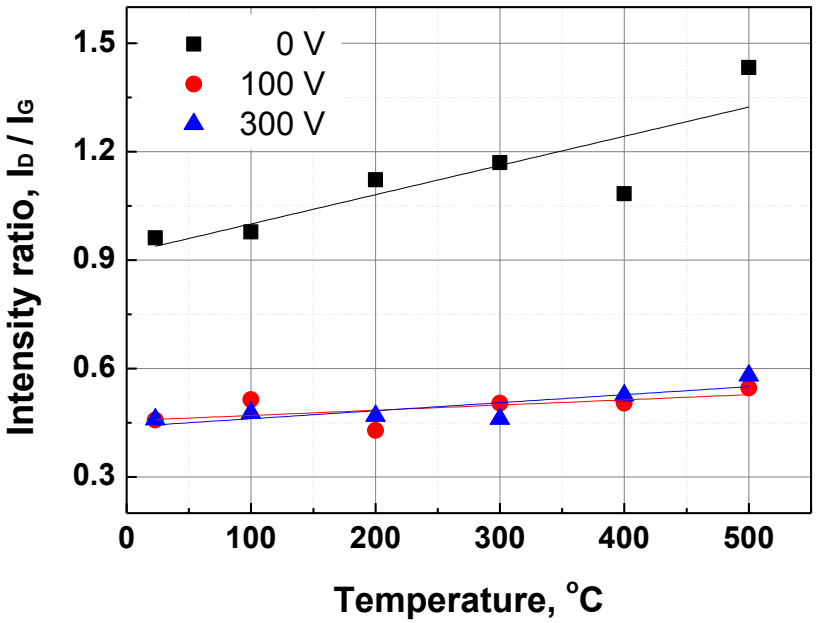

Figure 2.12. I_D/I_G ratio deconvoluted by Raman spectrum measured on the inside of wear track of ta-C coating.

2.3.4 Discussion

2.3.4.1 Effect of temperature on structure of ta-C coating and formation of transfer layer

The tribological behavior at high temperature is different from that at room temperature. The three coatings showed maximum wear rate at 300 ℃ for 0 V ta-C coating and at 100 ℃ for 100 V, 300 V ta-C, but wear rate did not further increase with increasing test temperature. These can be explained by hydrogen depletion, graphitization and formation of the transfer layer. The friction coefficient values of ta-C coating sliding against Si_3N_4 ball tested at 23 ℃ were slightly higher than those of higher temperature over 100 ℃ but showed stable friction behavior with a shorter running-in cycles. At 23 ℃, no transfer layer was developed on the counterpart materials. In Fig. 2.10, the blue area on wear scar of the Si_3N_4 ball tested at 23 ℃ looks like a transfer layer, but it is only identified as the Si_3N_4 peak from previous research by Deng [53]. These low friction tested at 23 ℃ were attributed to the presence of -H, -OH and water molecules dissociated from moisture in the ambient air [86,91,92]. In the surrounding atmosphere, the dangling bonds can be covered with -H, -OH and H_2O molecules on the topmost surface of ta-C coating and Si_3N_4 ball. The carbon dangling bond passivated by -H, -OH, and H_2O molecules can decrease covalent bonds and friction force between the sliding interfaces.

Importantly, upon heat to 100 ℃, longer running-in cycles in the initial part of friction coefficient were maintained and then lower friction coefficient was shown at steady state region at 100 ℃ than that at 23 ℃. In Fig. 2.9, the wear rate of 0 V, 100 V and 300 V ta-C coating tested at 100 ℃ increases approximately 10 times compared to that at 23 ℃. The high wear rate of ta-C coating depends on the counterpart material as shown in Fig. 2.9. In previous research, these severe wear rate with longer running-in cycles shown at testing temperature over 100 ℃ have a strong dependence on the depletion of surface passivating groups [53,56]. At 100 ℃, the dangling bonds of ta-C coatings and Si_3N_4 ball surface are no longer passivated, which lead to strong covalent bond between sliding surface. The strong covalent bond causes the high adhesion and initial friction force good agreement with the longer running-in cycles. In additional, ball surface may be quickly polished with higher wear rate.

In the structural evolution of ta-C coating as shown in Fig. 2.12, the running-in cycles began to decrease and the transferred layer steadily was formed on the counterpart material over testing temperature of 300 ℃. Graphitized transfer layer covered the contact area of wear scar on the ball and was clearly observed at the center of the wear scar as depicted in Fig. 2.10. From the Raman spectra shown in Fig. 2.11, it was confirmed that separation of G peak and the D peak were higher with increasing I_D/I_G ratio, implying that graphitization further progressed as the temperature was

increased [90]. Thick transfer layer was formed. With reducing strong covalent interaction, wear rates in 100 V and 300 V ta-C coating was decreased and prevents to further increase of wear rate of 0V ta-C coating over the 300 ℃ .

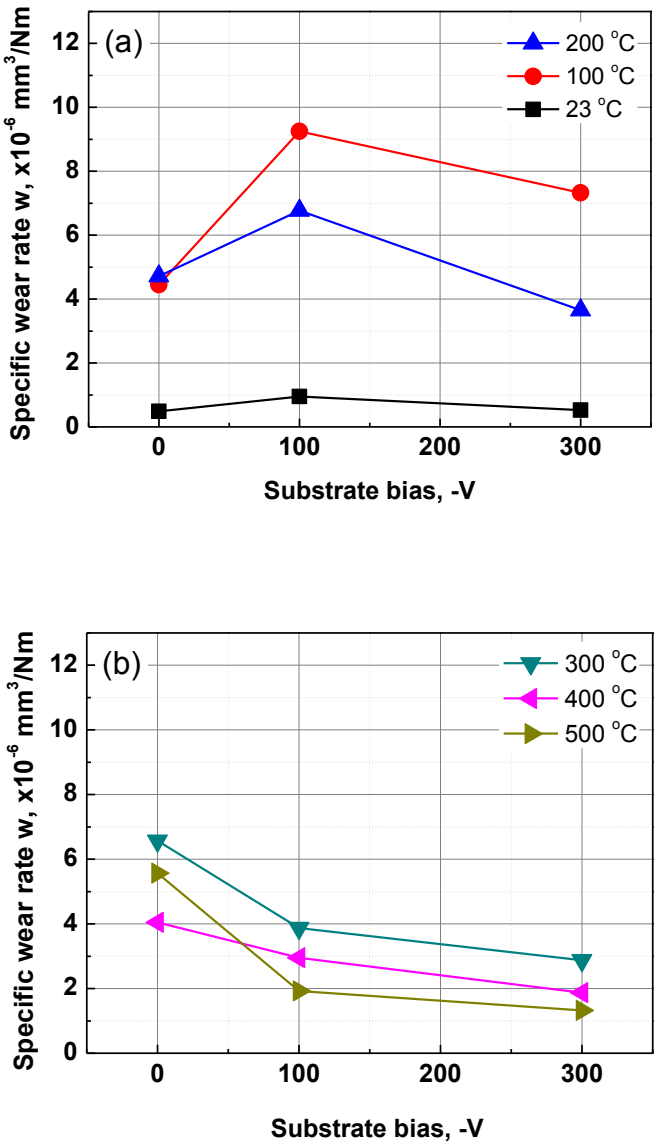

Figure 2.13. Specific wear rate of ta-C coatings deposited by different substrate bias as a function of bias with a different temperature from (a) Region Ⅰ: 23 to 200 ℃, (b) Region Ⅱ : 300 to 500 ℃.

2.3.4.2 Effect of substrate bias on wear behavior

From the effect of temperature, hydrogen depletion began at 100 ℃ and structural change of the coating and formation of transfer layer on wear scar of ball proceeded over 300 ℃. Wear behavior tested at same temperature showed different as a function of substrate bias. Wear rate of ta-C coating was replotted as a function of substrate bias as indicated in Fig.2.12 to explain the relationship between wear behavior at high temperatures and substrate bias.

Wear mechanism was illustrated in Fig.2.13 and the wear behavior can be divided into two categories: Region Ⅰ at 23, 100 and 200 ℃ ; Region Ⅱ at 300, 400 and 500 ℃. In the Region Ⅰ where transfer layer as a protective layer between ta-C coating and counterpart material did not form stably, it seemed that the coating surface was dominantly damaged by wear debris and abrasive particles. Hardness of the abrasive particles and debris appears to be proportional to the hardness of the coating because the particles are occurred from the surface of coating. The 100 V ta-C coating presents a much higher wear rate with a longer running-in cycles despite of having higher hardness of ta-C coating. This severe wear with longer running-in cycles agrees well with previous reports [56,85,93]. During the running-in cycles, the abrasive particles generated from the surface of 100 V ta-C coating with higher hardness results in severe wear with disturbing to form a transfer layer on the wear scar.

In the Region Ⅱ, sufficient softening occurred on the top surface in a short time, so that the transfer layer was easy to form on the counterpart. After that, in the steady state it seems that sp^3 content in its structure, which has a strong influence on the structural and mechanical properties of ta-C coating, is the main variable on wear behavior. The resistance to structural change of ta-C coating that led to decrease of sp^3 bond and increase of sp^2 bond in its structure can be confirmed by the slope of the I_D/I_G ratio shown in Fig. 2.12. The I_D/I_G ratio of 0 V ta-C had a large slope with increasing temperature, which means that further graphitization has progressed. On the other hand, at 100 and 300 V ta-C coating, the slope is small, which means that the graphitization has progressed less, and it is inferred that the sp^3 content is further maintained even at a high temperature. Therefore, it seems that at higher temperatures above 300 ℃, the higher wear resistance and decrease of wear rate at 100 V and 300 V ta-C coating was attributed to maintain of the sp^3 bond in its structure.

Substrate bias affects the structural, physical, and mechanical properties during the deposition process. Increase of the substrate bias to 100 V increases the sp^3 content in the ta-C coating structure, thereby improving the physical and mechanical properties. The ta-C coating deposited at substrate bias of 100 V, the wear resistance was poor due to effect of abrasive particles during the friction at the test temperature from 23 to 200 ℃. As the temperature increased over 300 ° C, the graphitization on

the surface progressed, and it was confirmed that this improved the wear resistance by helping to form transfer layer on counter-part material. An additional increase of substrate bias up to 300 V resulted in a graphitization of the surface due to the higher impact energy than the increase in sp^3 content in ta-C structure, which slightly reduced the mechanical properties rather than the ta-C deposited at 100 V, but the tribological properties were improved due to the graphitized surface.

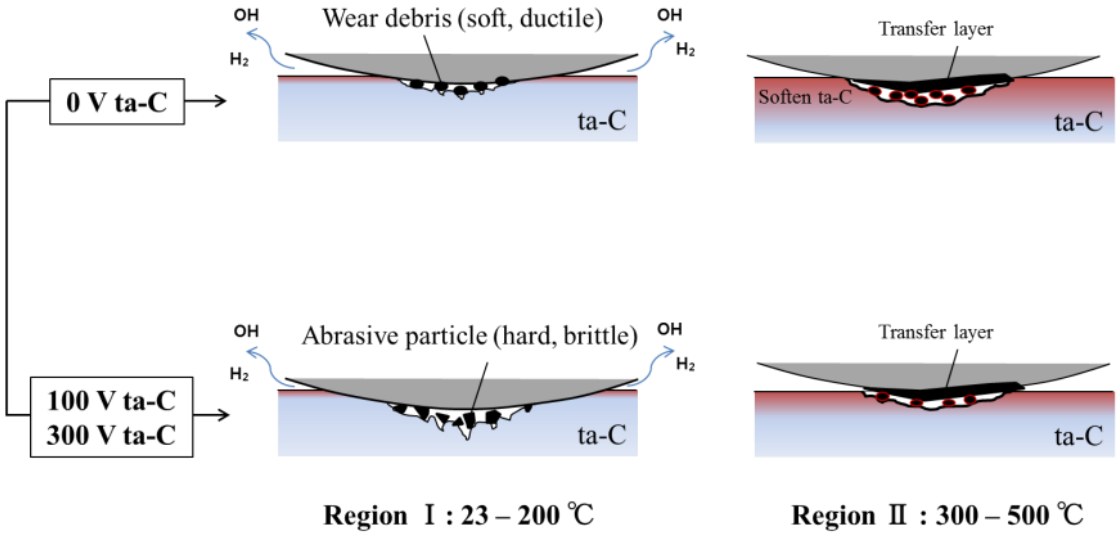

Figure 2.14. Schematic of wear mechanism at elevated temperature.

2.4 Conclusion

This study reveals the relationship among structural change, carbonaceous transfer layer and tribological behavior of ta-C coating deposited with a different substrate bias of 0, 100 and 300 V at elevated temperature.

- Increasing temperature leads to not only structural change of ta-C coating from sp^3 to sp^2 but also promoting formation of carbonaceous transfer layer on Si_3N_4 ball. Steady state friction coefficient decreased from 0.2 to 0.08 after formation of transfer layer.

The wear rate was categorized into two distinct regions.

- In region Ⅰ at 23, 100 and 200 ℃, highest wear rate appears at testing temperature of 100 ℃. The 100 V ta-C coating severely wears due to the abrasive particles with highest sp^3 content.

- In region Ⅱ at 300, 400 and 500 ℃, specific wear rate decreased with increasing substrate bias. Content of sp^3 was similar in 100 and 300 V ta-C coatings compared to 0 V ta-C coatings, which explain reduction of specific wear rate with an increase of substrate bias after 300 ℃. Thick transfer layer with graphitization is prevented from high friction and wear.

Chapter 3
Running-in behavior and understanding wear behavior of ta-C coating with filtered cathodic vacuum arc deposition

3.1 Introduction

Diamond like-carbon (DLC) coatings have been attracting considerable attention due to their superior mechanical and tribological properties. DLC coatings are a form of amorphous structure that contains sp^2 bonded graphite structure and sp^3 bonded diamond structure. The DLC coating was categorized into the hydrogenated diamond-like carbon and non-hydrogenated amorphous carbon with a content of hydrogen and sp^2/sp^3 ratio [55,89,94,95]. Among the DLC series, ta-C coating was a good candidate as a protective coating to the tribological application demanding to the superior durability and low friction properties at high temperature condition [66,96,97]. Especially, ta-C coating deposited by FCVA technique have a great attention in various fields such as infrared optical system, bio-medical application and auto-mobile component due to the high chemical inertness, mechanical and low frictional properties [30,98,99]. However, by using this arc method, ta-C coating with

high sp^3 content is possible by supplying highly ion energy to carbon ions, but at the same time it is reported that the generation of macro particles adhere to base material are inevitable.

In this regard, it is important micro structure of ta-C coating which is relationship between coating durability and performance of application. In additionally, the durability of ta-C coating depend on the surface roughness, defect like a pinhole and temperature. In previous research, many studies have been carried out to reveal the relationship between DLC coatings and wear properties. Mabuchi et al. [100] reported the effect of the dropping out of droplets on ta-C coating fabricated by FCVA method under a lubricated condition. Drescher et al. [67] showed the morphology and structural properties of DLC films deposited by Laser arc arrangement. Takikawa et al. [62] analyzed the droplets generated during the deposition process using T-FAD system and suggest the minimization method of droplets. Dorner et al. [68] deposited DLC coating with a different thickness and characterized the structural and durability of DLC coating as a function of coating thickness. In the view of removal of macro particles, many studies have been investigated to reduce the macro particles called droplets. Some studies have attempted to remove mechanical filters. In another study, application of curve duct and magnet field was proposed. However, as the curve angle increases, the deposition rate decreases. Therefore, it is suggested to use FCVA with

45^{o} curved duct and mechanical filter as a compromise.

When fabricating ta-C using this FCVA method, it is possible to fabricate high quality ta-C by decreasing the mirco particle with a relatively high deposition rate. There are few investigations for effect morphology and defects in ta-C coating on wear and friction behavior. Therefore, this chapter describes the influence of defect and role of transfer layer on the friction and wear behavior which is able to help in designing wear resistance coatings applied at high temperature condition. Tribological behavior of ta-C coated disk against Si_3N_4 ball was conducted at high temperatures of 200 ℃ with different sliding cycles. In order to confirm the effect of defects in ta-C on tribological behavior, defect in ta-C surface in designated area was investigated and compared the morphology, structure and friction and wear behavior at high temperature condition.

3.2 Experimental details

3.2.1 ta-C coatings and counter materials

The ta-C coatings investigated in this study were deposited on Inconel by using a FCVA system with a 45° curved filter employed to remove all unwanted macro-particles. A substrate holder was rotated at a constant speed for uniformity with the exit of FCVA source to substrate of 15 cm. Prior to the deposition, the substrate

was thoroughly cleaned ultrasonically in alcohol and de-ionized water. The deposition base pressure was below 5×10^{-3} Pa. Before deposition, argon ion beam bombardment was employed to remove the oxide layer and impurities on surface of the silicon and Inconel disk composed with nickel (68 %), chrome (17 %) and iron (8 %). Inconel disk is well suited for this study requiring high strength and good corrosion resistance in high temperature due to investigating tribological behavior of top surface of ta-C coating. A chromium layer was deposited to enhance the adhesion between the substrate and ta-C coatings. The deposition was carried out at an applied an arc current of 60 A and negative substrate bias voltage of 100 V.

3.2.2 Tribological experiments

The tribological performance of ta-C coatings was confirmed by using a high-temperature ball-on-disk type tribo-tester to evaluate the friction. These specimens were preheated 200℃, in ambient air via an Infrared lamp and temperature was maintained at the set value during the friction test. A silicon nitride (Si_3N_4) ball (Φ=8 mm) was used as a counter-part material with the wear track radius of 3 mm. For each test, a load of 1 N was applied on a Si_3N_4 ball rotating at a sliding speed of 200 rpm until completion of 2000, 4000, 8000 and 12000 cycles, respectively. The microstructure of the wear tracks on the coating and wear scars on Si_3N_4 ball were

measured by using Raman spectroscopy (Jasco, NRS-1000), with 532 nm laser and examined by Scanning electron microscope (SEM) and optical microscopy. To calculate the cross-sectional of wear tracks measured by Non-contact surface profiler (ZYGO, Newview6200), an average of four different measurements was used.

After friction tests, wear scars of balls and disks were observed using optical microscopy. Since the wear volume (V), estimation of disk side could not be achieved, wear rate calculation was only conducted on coated ball side. The specific wear rate (mm^3/Nm) was calculated using the Archard wear equation given by

$$\text{specific wear rate} = \frac{V}{W \times L} \quad , \tag{3.1}$$

where W is the normal load (N), and L represents sliding distance (m). Raman spectroscope measurement (Jasco NRS-1000 Laser) was also performed on the wear scars to identify the transfer layer. The thickness and surface roughness of transfer layer was confirmed by Optical microscopy and 3D measuring laser microscope (Olympus, LEXT OLS5000)

3.3 Results

3.3.1 Tribological performance of ta-C coating

Figure 3.1 showed friction coefficient of the ta-C coatings fabricated with a substrate bias voltage of -100 V up to sliding cycles of 12000 under temperature of 200 ℃. In this experiment, ta-C coating exhibited a running-in cycles and then the steady state (μ_s=0.02) was reached after 2000 cycles. The other result with a different number of cycles of 4000, 8000 and 12000 showed similar behavior that the running-in cycles was maintained up to 2000 cycles and steady state was obtained as a result of 12000 cycles.

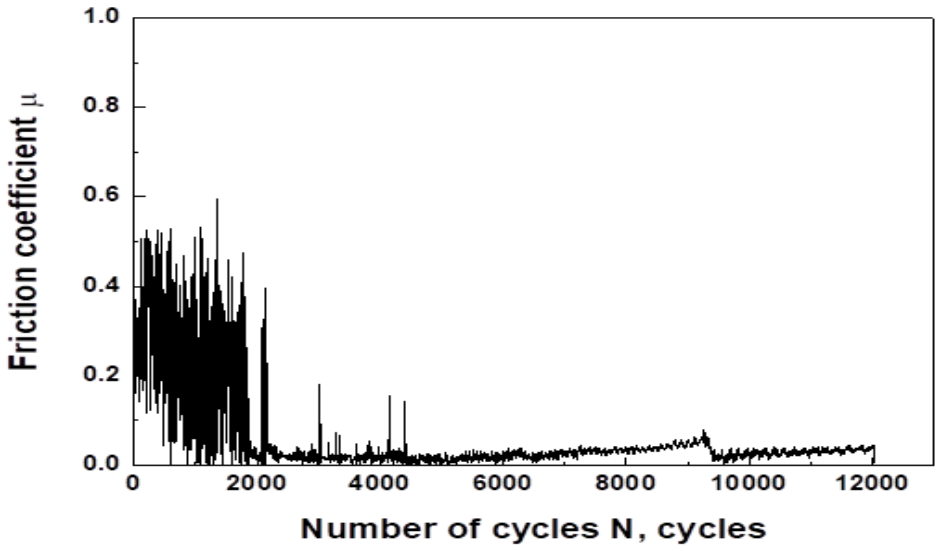

Figure 3.1. Friction coefficient of ta-C against the Si_3N_4 ball at 200 ℃. Tests were run for 12000 cycles using 1 N applied load at 200 rpm.

The combined two-dimensional cross section image of wear track of ta-C coating for 2000, 4000, 8000 and 12000 cycles are shown in Fig. 3.2 (a). At 2000 cycles, wear track of ta-C was considerable with apparent damage surface. Up to the 2000 cycles, a fluctuation of friction coefficient was maintained with a higher wear. However, the depth of wear track became slightly deeper with an increase of sliding cycles. A Specific wear rates can be calculated using the cross-sectional wear area with length of wear track and applied load. The wear rate of the 4000, 8000 and 12000 cycles was calculated except to the wear volume occurred in 2000 cycles to confirm the effect of the transfer layer on the ball on wear behavior. The ta-C film exhibited a higher wear rate of 9.6×10^{-6} mm^3/Nm at 2000 cycles. However, wear rate started to be sharply decreased to 6.0×10^{-7} mm^3/Nm at 4000 cycles and then reached to the 2.5×10^{-7} mm^3/Nm at 12000 cycles as shown in Fig. 3.2 (b).

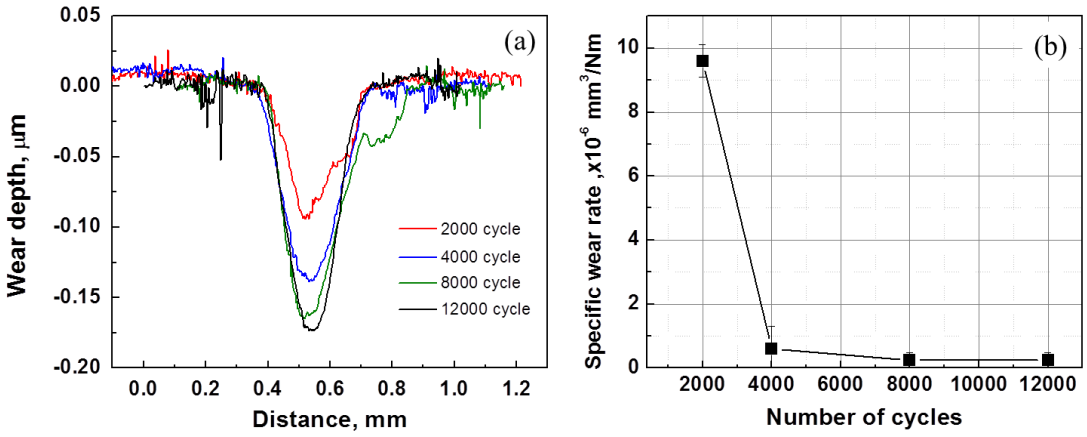

Figure 3.2. (a) Combined cross-sectional image of wear track, (b) specific wear rate of ta-C coating as a function of number of cycles.

3.3.2 Morphology of ta-C coating

Fig. 3.3 (a) shows surface morphology of ta-C coating measured by SEM micrograph. Through the SEM image, pores and nodular defects of various shape and sizes were visible. Some of nodular defects called as Droplets looked like that macro-particles were embedded in ta-C matrix. The sized of nodular defects varied around an average value of 0.7-1.0 μm. There were probably also some pores formed when the solidified droplets break off after the deposition process has been completed. Some pores with various diameters of 0.05-10 μm were present.

To confirm the effect of defects on tribological behavior, surface morphology at designated area was compared with increasing different sliding cycles. After 1000 cycles, change of surface morphology in wear track in ta-C coating was observed. It is notice that top of nodular defects were polished but were remained inside of wear track as presented in Fig. 3.3 (b). Then nodular defects were almost grinded off and pores were damaged and scratch grooves by abrasive wear was confirmed behind the sliding direction displayed in Fig. 3.3 (c). Especially, these changes of morphology could be seen more clearly in enlarged SEM image shown in Fig. 3.4.

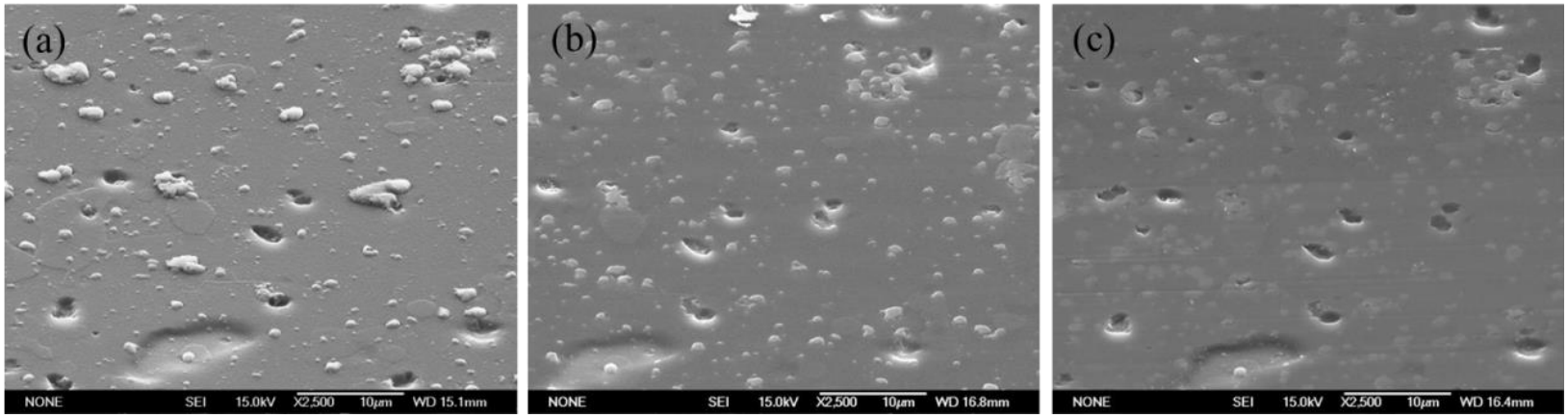

Figure 3.3. SEM image of wear track at a different sliding cycles at (a) 0 cycles, (b) 1000 cycles (c) 4000 cycles.

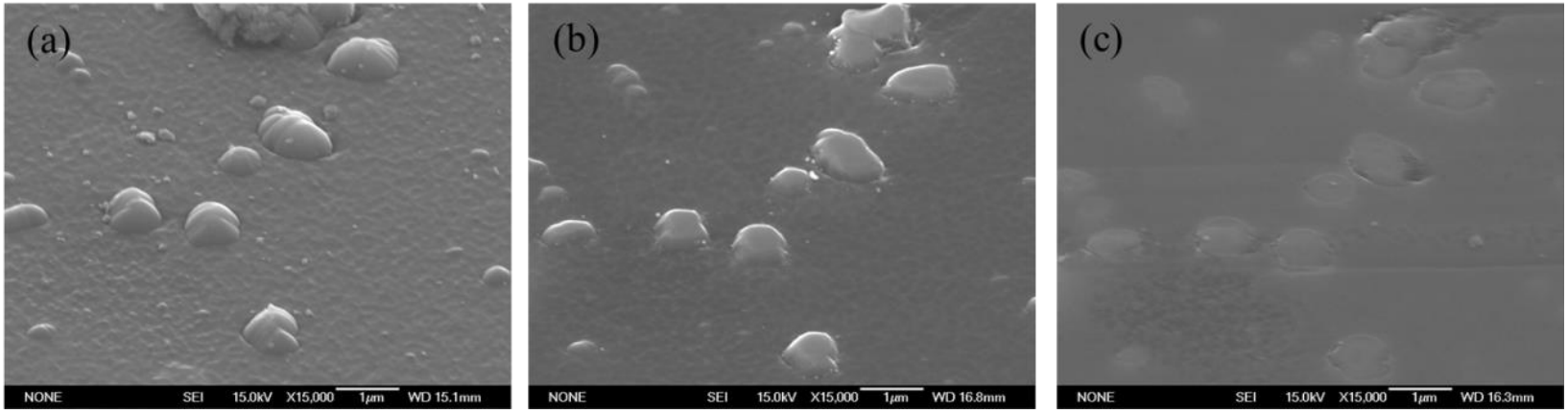

Figure 3.4. Enlarged SEM image of wear track at a different sliding cycles at (a) 0 cycles, (b) 1000 cycles and (c) 4000 cycles.

3.3.3 Analysis of tribo-layer

After the friction test, there were clearly noticeable wear scar on surface of the Si_3N_4 ball. Figure 3.5 (a) shows the optical image of wear scar on the Si_3N_4 ball in the contact area at 2000 cycles. It is obviously seen that wear scars, partially covered by colourful layer with a rough surface, formed on the Si_3N_4 ball. There was an accumulation of carbon debris in front of wear scar. At 4000 cycles, these were noticeable integrity tribo-layer formation with a partial buckling and an amount of wear debris was accumulated as shown in Fig 3.5 (b). Further increase of sliding cycles up to 12000 cycles, tribo-layer could be seen on wear scar without bucking compared to that at 4000 cycles (Fig 3.5 (c)). The diameters of wear scars did not increase with variation of sliding cycle up to 4000 and 12000 cycles.

In order to confirm the carboneous tribo-layer on wear scar and explain the tribological behaviour with a formation of transfer layer, Raman analysis was conducted. Figure 3.6 shows the Raman spectrum of ta-C coating, Si_3N_4 ball and graphitized transfer layer on wear scar of Si_3N_4 ball against ta-C coating with sliding cycle of 4000 cycles. In the case of graphitized transfer layer on Si_3N_4 ball, the D peaks around 1350 cm^{-1} and G peaks around 1580 cm^{-1} was separated meaning that the graphitized transfer films are formed wear scar.

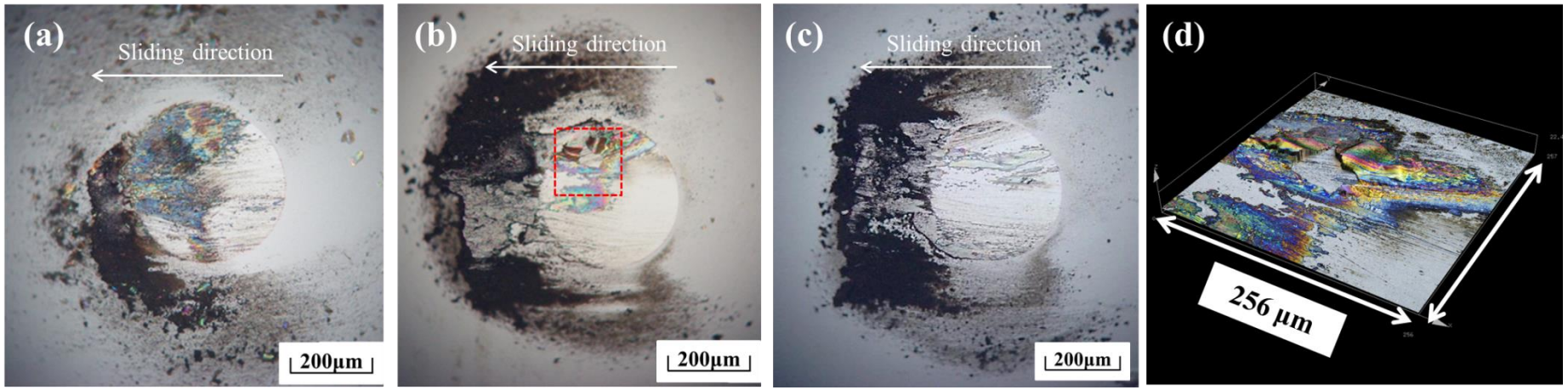

Figure 3.5. Wear scar on the ball at different sliding distance of (a) 2,000, (b) 4,000 and (c) 12,000 cycles. (d) Enlarged 3D image of transfer layer indicated in red dot square in Fig. 2 (b) showed a buckling on Si_3N_4 ball.

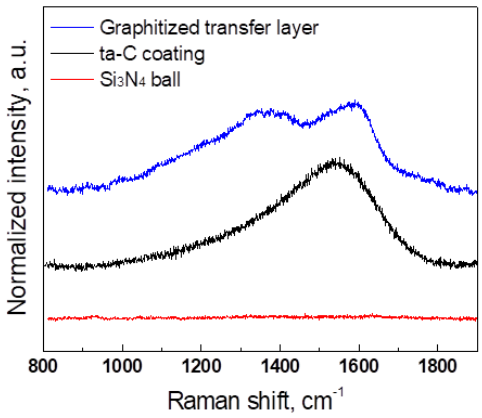

Figure 3.6. Raman spectrum of Silicon nitride, as-deposited ta-C coating and graphitized transfer layer on the wear scar after testing up to 4000 cycles.

The Raman spectra of carbon debris accumulated in front of sliding direction, colourful layer presented on the wear scar and polished surface was investigated, shown like Fig. 3.7. The Raman spectra in Fig. 3.7 (a) show a characteristic of graphitized transfer layer in the carbon debris and colourful tribo-layer. The appearance of D peak at 1350 cm^{-1} with a low intensity in the Raman spectra on the carbon debris and colourful layer indicated an increase of sp^2 bonds with a change in the bonding structure of the surface of ta-C coating and small size of cluster.

However, polished surface beside the transfer layer only indicated the Si_3N_4 peak [53]. Further increase of sliding cycles until 4000 cycles, higher intensity of Raman spectrum was shown compared to that up to 2000 cycles. Carbonaceous transfer layer was could be seen not only at colourful layer but also polished area until 12000 cycles. From this observation, it was obviously seen that wear scars was partially covered by carboneous transfer films in initial term. During steady state wear scar was overall

covered by transfer layer with smooth surface as a thicker film and maintains a thickness of approximately over 200 μm as shown in Fig. 3.8.

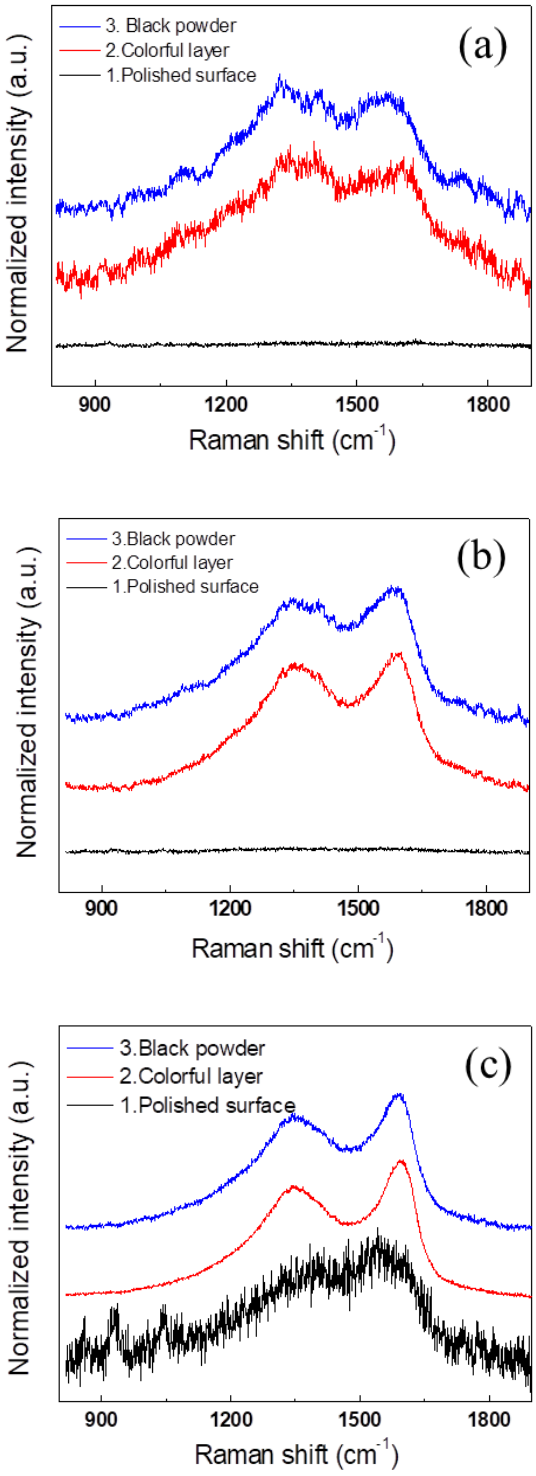

Figure 3.7. Raman spectrum of carbon debris, colorful layer and polished surface on the wear scar after testing up to (a) 2000 cycles, (b) 4000 cycles (c) 12000 cycles.

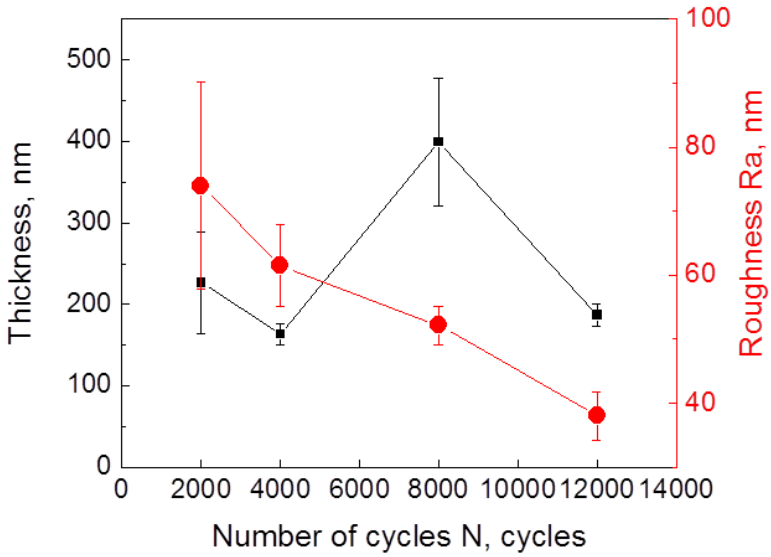

Figure 3.8. Comparison between thickness and roughness of transfer layer as a function of sliding cycles.

3.4 Discussion

Understanding the role of the running-in behaviors and the mechanism of transfer layer formation on the counterpart material are important to assure the thermal stability of ta-C coating. To explain the tribological behavior conducted at 200 ℃, morphological and structural properties of ta-C coating were confirmed. On the basis of SEM microscopy (Fig. 3.3 (a) and Fig. 3.4 (a)), a lot of defects was observed on the ta-C surface.

To explain the effect of those defects on friction and wear properties, wear mechanism was proposed as schematic image expressed in Fig. 3.9. As shown in Fig. 3.9 (a), nodular defects were survived during the sliding. It seem to be the main

reason for the running-in cycles at the beginning of the 2000 cycle with disturbing to form the tribo-layer on the counter-part material and rough surface of tribo-layer formed on counter-part material estimated from Raman spectrum illustrated in Fig. 3.7 (a). In the middle of sliding, transfer layer formed on wear scar of Si_3N_4 ball was peeling off by the nodular defects. At the same time, abrasive particles spalled off nodular defects result in the severe wear at sliding interface shown in Fig. 3.9 (b).

In additional, it were reported that hydrogen and water molecules covered with the contact surface on the ta-C film and counter-part material was released under the high temperature [91,101]. Covalent interactions on the unsaturated surface between the ta-C coating and Si_3N_4 ball result in running in cycles and higher wear rate until the 2000 cycles as a process of formations of carbonaceous transfer film.

From the optical image of wear scar (Fig. 3.5 (b)) and Raman spectrum (Fig. 3.7(b)), these are clearly noticeable formation of transfer layer corresponding to the low friction coefficient (0.02 shown in Fig. 3.1) and lower specific wear rate after 2000 cycles. Due to the presence of transfer layer formed on the wear scar on the ball, it is enough to passivate dangling bond generated at high temperature condition with a decreasing a shear strength and a protection of both ta-C film and counterpart material as illustrated in Fig. 3.9 (c).

Next, the graphitized transfer layer on counterpart materials is an important role of

wear behavior. To transfer the carbonaceous tribo-layer on the Si_3N_4 ball from ta-C coating, graphitized carbon debris was accumulated in front of sliding direction. In an initial term up to 2000 cycles this transfer layer was composed of small size of cluster with rough surface. After that, transfer layer was stably formed with thicker type of tribo film and covering the whole of wear scar on the Si_3N_4 ball.

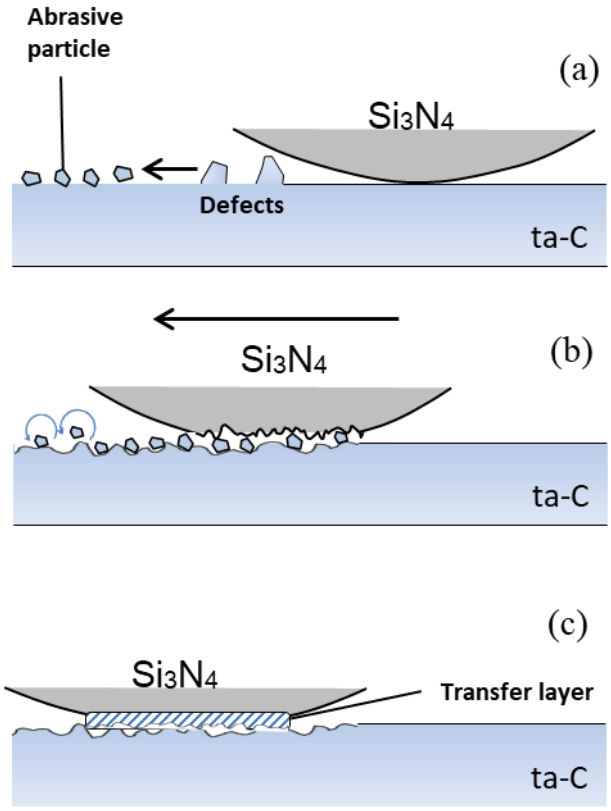

Figure 3.9. Schematic of wear mechanism at different sliding cycles ; (a) as-deposited, (b) running-in cycles up to 2000 cycles and (c)steady state from 2000 to 12000 cycles

3.5 Conclusions

The study presented the tribological behaviors of ta-C coating versus Si_3N_4 ball at high temperature of 200 ℃ as a function of sliding cycles. Tribological behaviors at high temperature are appeared in by morphology of ta-C coating surface and transfer film formation.

- Running-in cycles shown up to 2000 cycles removed nodular defects and then specific wear rate was sharply decreased during the steady state region.
- Low friction coefficient of 0.02 and low wear rates of $2.5x10^{-7}$ mm^3/Nm were observed at 12000 cycles. The steady state friction coefficient and decrease of wear rate were attributed by the formation of transfer layer on the wear scar of the Si_3N_4 ball.
- This graphitized transfer layer around thickness of 300 nm can significantly protect the ta-C coating surface with covering whole area of Si_3N_4 surface.
- Higher wear rate was correlated with running-in cycles as a process of formations of carbonaceous transfer film.
- The results demonstrate that transfer layer formation influence tribological behavior decreasing the interaction between ta-C films and wear scar on the Si_3N_4 sphere.

Chapter 4
Effect of defects on wear behavior in ta-C coating prepared by filtered cathodic vacuum arc deposition

4.1 Introduction

Tetrahedral amorphous carbon (ta-C) coatings have proven to be good candidates as protective coatings for tribological applications. Ta-C coating has attracted significant attention in various fields such as infrared optical systems, biomedical applications, and automobile components owing to its high percentage of sp^3 ratio, a very high density and highly transparent properties at infrared region.

Particularly, the ta-C coating can be reliably fabricated by the filtered cathodic vacuum arc (FCVA) technique. FCVA can produce ta-C coatings with high sp^3 content by supplying high energy to the carbon ions; however, inevitably, macroparticles adhere to the base material. It is important to understand the relationship between the coating durability and application-specific performance of ta-C coatings, in terms of the microstructure of the coating. The durability of ta-C coatings depends on the surface roughness, defects (like pinholes), and temperature. Many previous studies

have elucidated the wear properties of DLC coatings [62,68,81,100]. Many studies have attempted to remove microparticles occurring as droplets; some used mechanical filters of a curved duct and magnetic field were employed. Drawback is that the deposition rate decreased. Microparticle removal was attempted via FCVA with a 45° curved duct and a mechanical filter with increasing angle of curvature. High-quality ta-C coatings could be prepared by reducing microparticles using a relatively high deposition rate. Effect of morphology and defects in ta-C coatings on their wear and friction behavior is lack of researches; to completely block the inflow of microparticles should be critically investigated. Therefore, in this study, the types of defects present on a ta-C coating prepared via FCVA were classified, and the tribological behavior of the coating was evaluated against a Si_3N_4 ball. In order to reveal the effect of defects in the ta-C coating on the tribological behavior, the defects in a designated area on the surface of the ta-C coating were investigated, and their morphology, structure, friction and wear behavior were compared under high-temperature conditions.

4.2 Experimental details

4.2.1 Preparation of ta-C coating

In this study, the ta-C coating was deposited on Inconel using a FCVA system. The FCVA deposition system incorporates a 45° curved filter to effectively remove unwanted micro particles with a high deposition rate. An Inconel disk is chosen as a substrate due to high strength and good corrosion resistance at high temperature when investigating the tribological behavior of the top surface of a ta-C coating. Inconel disk was composed of nickel (68%), chrome (17%), and iron (8%) with a thickness of 2 mm and a diameter of 20 mm. The Inconel substrate was pre cleaned by alcohol and deionized water in ultrasonic bath. Before deposition, the native oxide layer on substrate and impurities was etched by argon ion beam. A chromium layer was deposited as an interlayer on substrate. To ensure uniformity of structure and thickness of coatings, the substrate holder was rotated at a constant speed. The deposition was carried out at an applied an arc current of 60 A. The ta-C coating was deposited using a negative substrate bias voltage of 100 V to obtain highly sp^3 bond ta-C coating.

4.2.2 Coating characterization

A high temperature ball-in-disk tribotester was used to evaluating the tribological behavior. The test was conducted at 170 ℃ in ambient air using an infrared lamp, and

this temperature was maintained in all tests. A silicon nitride (Si_3N_4) ball (Φ=8 mm) was used as a counterpart material. For each test, a load of 1 N was applied on a Si_3N_4 ball rotating at a sliding speed of 200 rpm, until the completion of 10000 revolutions with a wear track radius of 3 mm.

Raman spectroscopy (Jasco, NRS-1000) using a 532 nm laser, as well as by scanning electron microscopy (SEM) and optical microscopy was used to characterize the microstructures of the wear tracks and wear scars on the coating and ball. The cross-sectional area of the wear tracks was measured at 4 different locations along the wear track using a non-contact surface profiler (ZYGO, Newview6200). The hardness of the ta-C coating was measured using a nano-indentation tester with 1000 μN (Elionix, ENT-1100a,).

4.2.3 Surface analysis

Wear scars of the coatings were studied using optical microscopy to quantify the specific wear rates, calculated by using the wear equation

$$\text{specific wear rate} = \frac{V}{W \times L} \quad , \tag{4.1}$$

, where V is the wear volume (mm^3), W is the load (N), and L is the sliding distance (m). Raman spectroscopy measurement (Jasco NRS-1000 and Renishaw) was analyzed on the defects to confirm the structure.

4.3 Results

4.3.1 Morphological and structural properties of defects on ta-C coating

Figure 4.1 shows the surface morphology of the ta-C coating obtained by SEM. Pores, droplets, and spikes of various shapes and sizes are visible. Droplets appearing like macroparticles are embedded in the ta-C matrix and are weakly bonded due to partial detachment at the droplet boundary. Pores may be form when the solidified droplets break off after the completion of deposition. Some pores with various diameters in the range of 0.05-10 μm are present. The spikes are observed in the micrograph. It is noticeable differ from the droplets in size and shape, despite the same convexity for both. The spikes are 0.7-1.0 μm in size. No boundary due to detachment is observed between the particles and ta-C matrix.

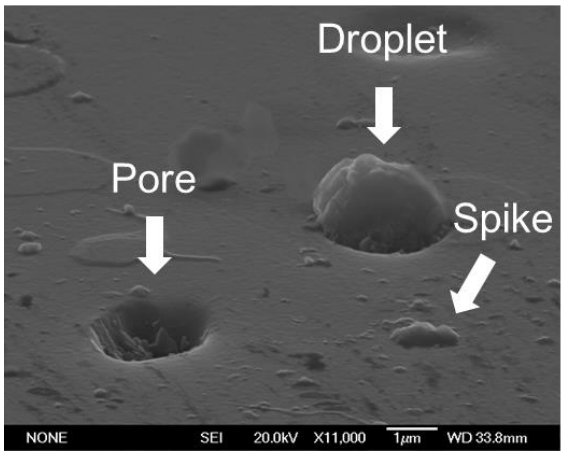

Figure 4.1. Typical SEM image of morphology of Defects composed with droplet, spike and pore on ta-C coating

To clarify the differences between the spikes and droplets, Raman spectroscopy was conducted. The Raman spectra of the defects and matrix of the ta-C coating were examined before and after the friction test at 170 ℃ (Fig. 4.2 (a)). Peak fitting provided detailed information; the spectrum of the ta-C matrix showed a characteristic broad amorphous peak, whereas defects in the form of droplets exhibited peaks nearly similar to those of graphite. The droplets appeared to be adhered to the substrate during the deposition. Pores without droplets exhibited a shoulder of the D peak at 1350 cm^{-1}, suggesting a sp^2-rich structure. The spikes were similar in structure to the ta-C matrix, but not the droplets. Table 4.1 shows the hardness values as well as the structural and morphological properties of the ta-C matrix and defects. Clearly, spikes with a cone-like shape possess superior structural and mechanical properties like the homogeneous ta-C matrix. Hence, it is expected that the spikes would affect the tribological behavior.

Table 4.1. Coating characteristics of ta-C coatings with a various negative substrate bias

Samples	Hardness, GPa	Young's modulus, GPa	Diameter, μm	Height or Depth, μm	I_D/I_G	G peak Position, cm^{-1}
Matrix of ta-C	52.2±2.8	568.0±24.0	-	-	0.460	1561.5
Spike	49.8±4.2	542.0±85.1	0.7-1	0.1-0.3	0.457	1563.2
Pore	3.0±1.4	94.6±28.3	0.05-10	0.02-0.68	2.227	1576.2
Droplet	7.0±4.3	102.3±52.1	1	0.3-0.5	0.116	1581.6

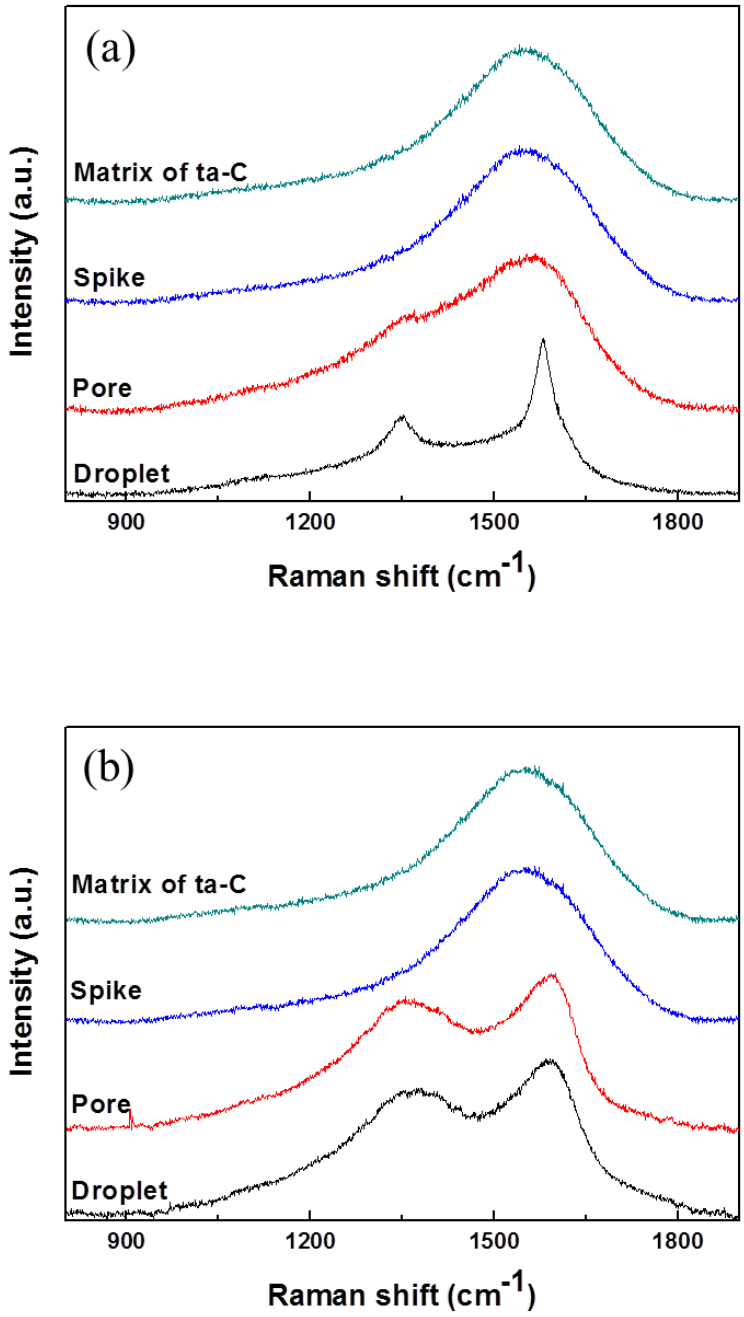

Figure 4.2. Raman spectrum, as measured at the center of matrix of ta-C, spike, pore and droplet (a) before and (b) after friction test at temperature of 170 ℃.

4.3.2 Tribological properties

In Fig. 4.3, the coefficient of friction of the ta-C coating is plotted against the number of sliding cycles (the sliding counterpart was a Si_3N_4 ball). Initially, a running-in cycle is maintained until 2000 cycles, following which a steady-state value of 0.1 is obtained. At the end of 10000 cycles, the wear rate of the ta-C coating is 4.3×10^{-6} mm^3/Nm. As shown in Fig. 4.4, the ta-C coating is grinded off near the 200 μm-wide wear track with wear debris.

The SEM images show spikes, droplets, and pores on the ta-C coating surface. Some spikes remain inside the wear track with a polished surface (Fig. 4.5). To confirm their effect on the tribological behavior, the surface morphology of the coating was compared before and after the friction test. Figure 4.5 shows the change in the morphology of the defects after the friction test. In Fig. 4.5 (a), the droplet is grinded off on top surface of that and is retained, and then the ta-C coating is behind the sliding direction up to sliding distance of 6000 cycles. On the other hand, the spikes are almost polished and there are only traces left as shown in Fig. 4.5 (b). In Fig. 4.5 (c), the boundaries of the pores are damaged, and scratch grooves due to abrasive wear are formed against the sliding direction.

In Fig. 4.2 (b), structural changes among the defects are apparent after the friction test at 170 ℃. For droplets possessing the same structure as graphite, the Raman

spectrum seems to be combined with graphite and DLC spectrum. For pores, the D peak occurs at 1350 cm^{-1}, implying that graphitization occurs at the pore. Finally, there are no major structural differences between the ta-C matrix and spikes.

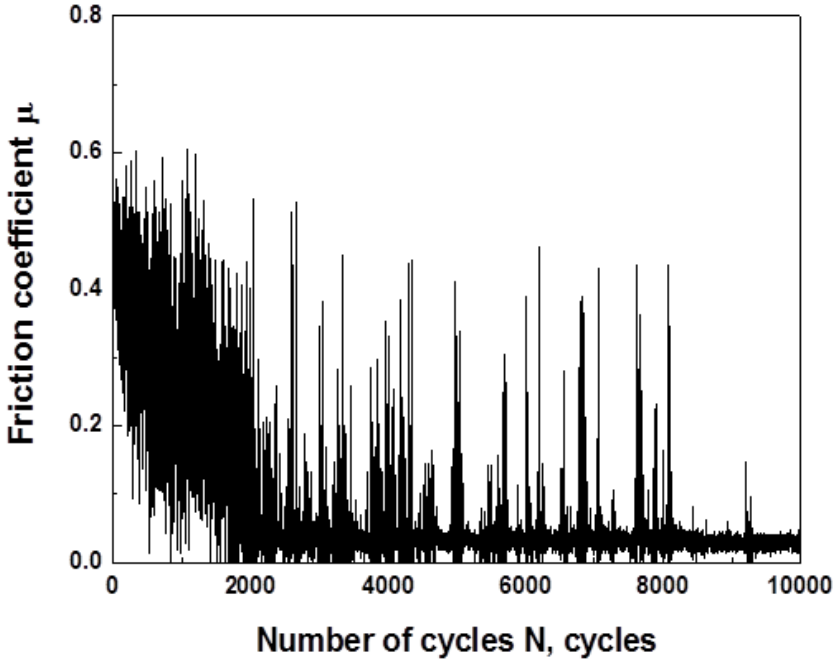

Figure 4.3. Variation of friction coefficient of ta-C coatings fabricated at a substrate bias of -100 V as a function of the number of sliding cycles at 170 ℃.

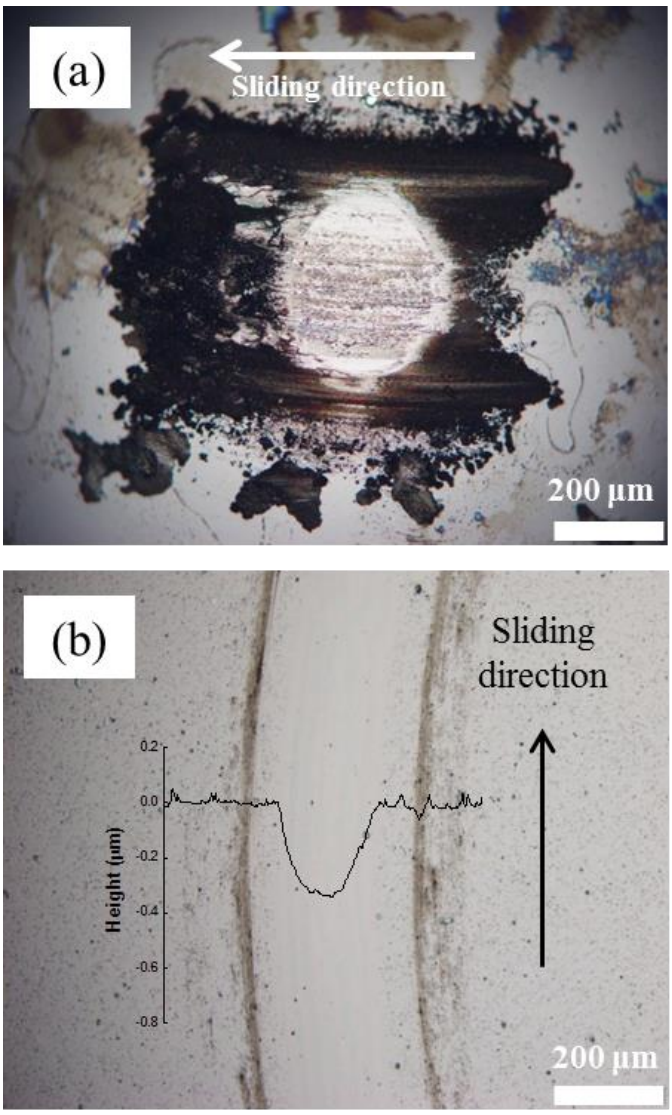

Figure 4.4. Optical microscope images of (a) the wear scar on the counterpart material(Si_3N_4) and (b) wear track combined with cross-sectional image of the ta-C coatings tested at temperature of 170 ℃.

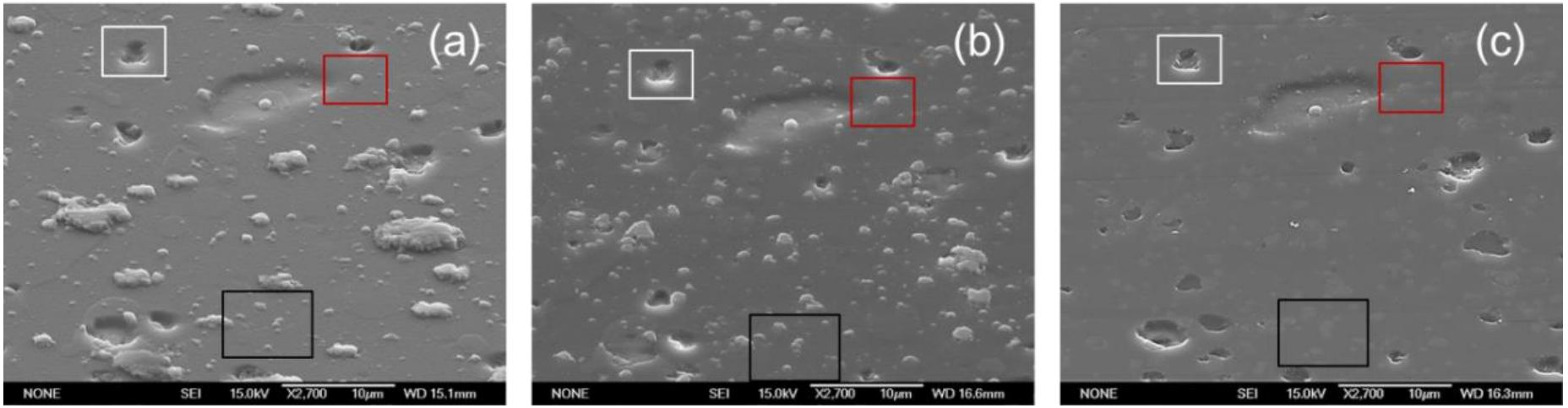

Figure 4.5. SEM micrographs of ta-C coating surface, (a)as-deposited surface and after (b)1000 cycles and (c)6000 cycles (red, black and white boxes represent droplet, spikes and pore, respectively)

4.4 Discussion

4.4.1 Classification of defects

To explain the tribological behavior at 170 ℃, the morphological, mechanical, and structural properties of the ta-C coating were analyzed. SEM images (Fig. 4.1) show numerous defects on the ta-C surface, which can be classified into droplets, pores, and spikes, depending on their morphology, size, and structure. Comparing the structure of graphite cathode materials with that of the droplet may reveal the origin of the droplet. Convex droplets embedded in the ta-C matrix possess the same Raman spectrum as typical graphite. Previous studies suggested that macroparticles in the form of droplets, which were generated from the graphite cathode material during deposition, were not filtered and subsequently adhered to the surface of the ta-C coating. This was unavoidable, because droplets are invariably produced during cathodic arc deposition. Among the defects, interestingly, the droplets showed wear. After the friction tests, some remnants were observed along the sliding direction inside the wear track. Field-emission SEM (FE-SEM) confirmed that with increasing sliding cycles, the droplets started to show wear behavior. In Fig. 4.6 (a) that enlarged views of Fig. 4.5, the top surface of the droplet is partially polished at 1000 sliding cycles. Upon increase in the sliding cycles to 6000, the droplet is deformed against the sliding direction and

wear occurs. Fig. 4.7 (a) shows the deformation of the droplet in the undesignated area inside the wear track, which is confirmed by AFM (Fig. 4.7 (b)). Unlike the spikes that grinded off, the deformation behavior of the droplets can be explained by the structure, which was confirmed by Raman analysis. The graphite structure in the droplets is similar to that in a DLC (termed "soft DLC") under the high-temperature friction test conducted at 170 ℃. Because of these soft and ductile properties, deformation occurs instead of grinding during the friction test.

The pores are approximately 1 μm in depth and size, like the droplets. These pores are in the form of cavities, whereas the droplets are weakly bonded to the homogeneous ta-C coating. Due to these "shadow effects", the droplets hinder the growth and structural uniformity of the coatings, leading to a rough, structurally non-uniform surface. Raman spectra indicate a shoulder of the D peak at 1350 cm^{-1}, implying the onset of graphitization or structural phase transformation from sp^3 to sp^2. Moreover, the increase in the intensity of the D peak for the pore is noticeable, implying that the phase transformation of the structure is accelerated upon the completion of the friction test at 170 ℃. On the other hand, for the spikes, the Raman spectra indicate no significant changes in the structure under the same condition of the friction test. Therefore, the spikes, though convex like the droplets, possess distinct structural and mechanical properties. From the structural and mechanical point of view, these spikes possess

properties similar to those of the ta-C matrix despite being convex, and hence, may affect the tribological behavior.

4.4.2 Wear mechanism on defective surface

The wear mechanism explaining the effect of the spikes on the friction and wear properties is illustrated in Fig. 4.9. At first, it disturbed to form the tribo-layer on the counter-part material. As shown in Fig. 4.6 (b), the spikes are retained during sliding. This appears to be primarily responsible for the longer running-in cycles at the start of the 2,000 cycle, due to which a rough tribolayer formed on the sliding counterpart. During sliding, a transfer layer formed on the wear scar of the Si_3N_4 ball was peeled off by convex spikes with high hardness, as shown in Fig. 4.9 (a). This provided abrasive particles, resulting in severe wear of the surface of the ta-C coating as well as at the sliding interface. Particularly, the pore where the structural transformation from sp^3 to sp^2 occurred, had a low hardness, and was damaged by these abrasive particles (Fig. 4.8 (a) and (b)) as illustrated in Fig. 4.9 (b) and (c). There are some studies explaining the origin and growth of these spikes. The seed of spikes comes from small particles at the graphite cathode target during deposition [102,103]. The seed of spikes was possibly provided by the sp^3-rich particles deposited on the edge of the baffle. It is easy to detach these particles from the baffle due to the high residual stress and low adhesion. The origin of the spikes needs to be further investigated, by which it will be possible to

suggest ways to minimize droplets and enhance the quality of the coating and thereby the tribological characteristics.

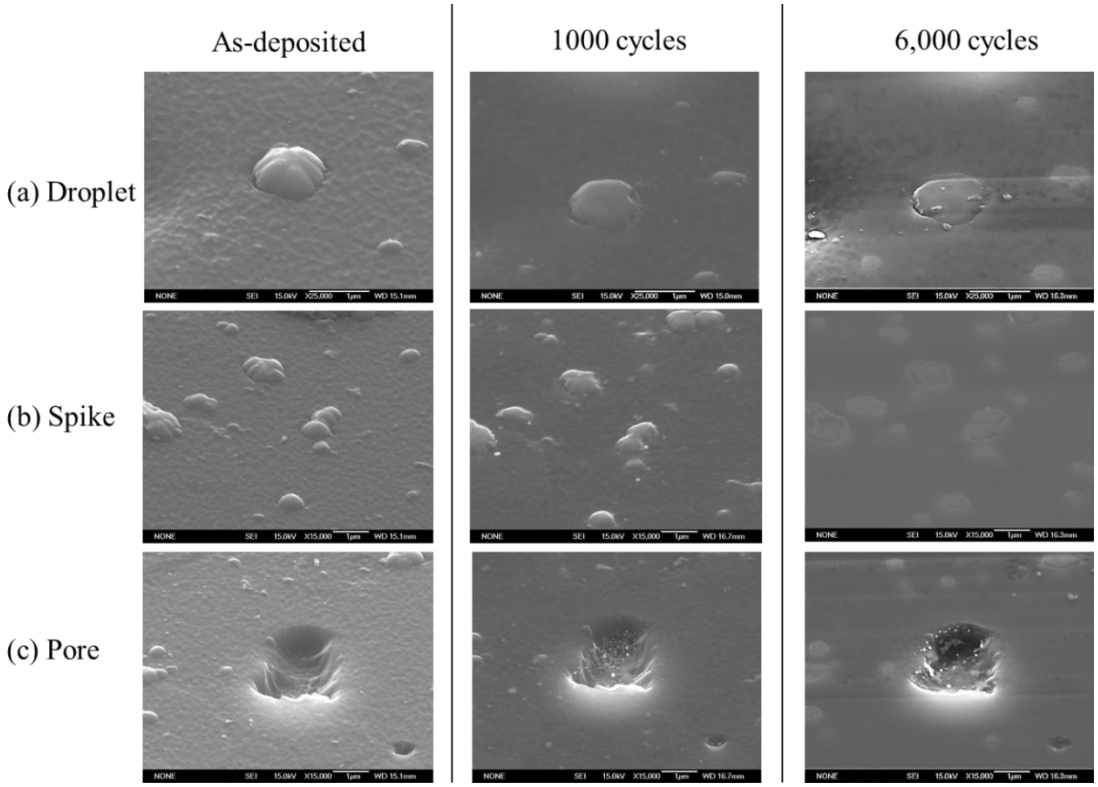

Figure 4.6. SEM image of (a) droplet, (b) spike and (c) pore at designated area marked in Fig. 4.5 as a function of different sliding cycles

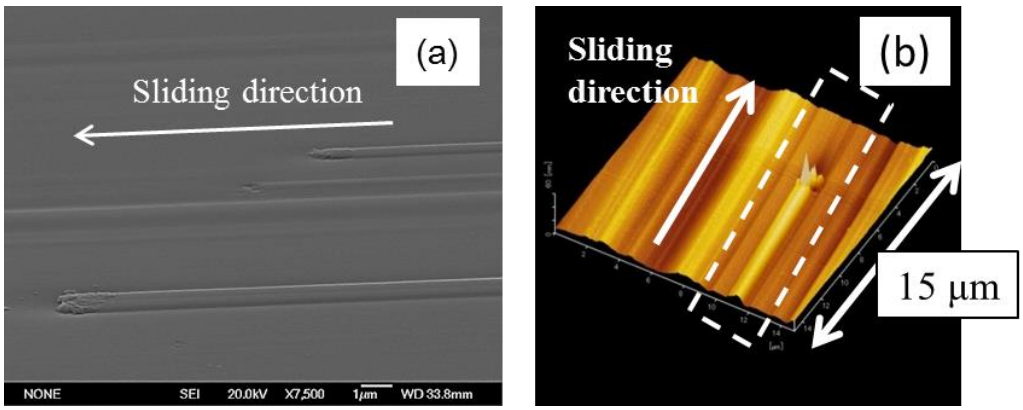

Figure 4.7. Droplet and deformed part along with sliding direction measured by (a)FE-SEM and (b)AFM

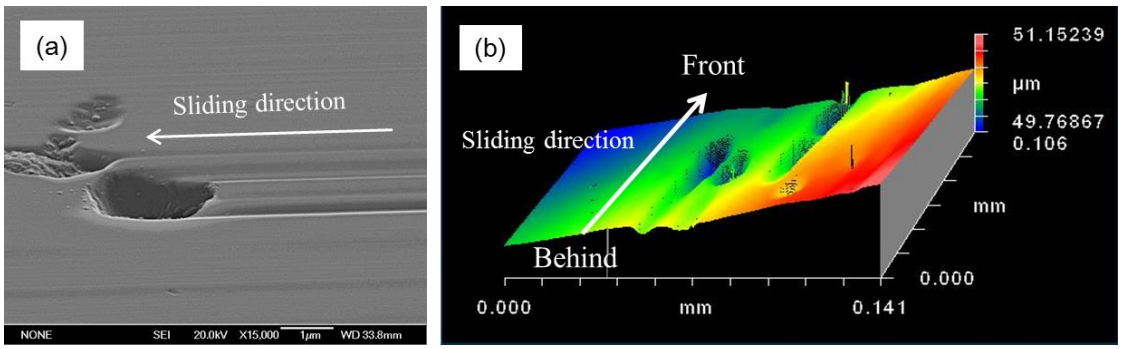

Figure 4.8. Pore and scratch grooves with sliding direction measured by (a)FE-SEM and (b)non-surface profiler

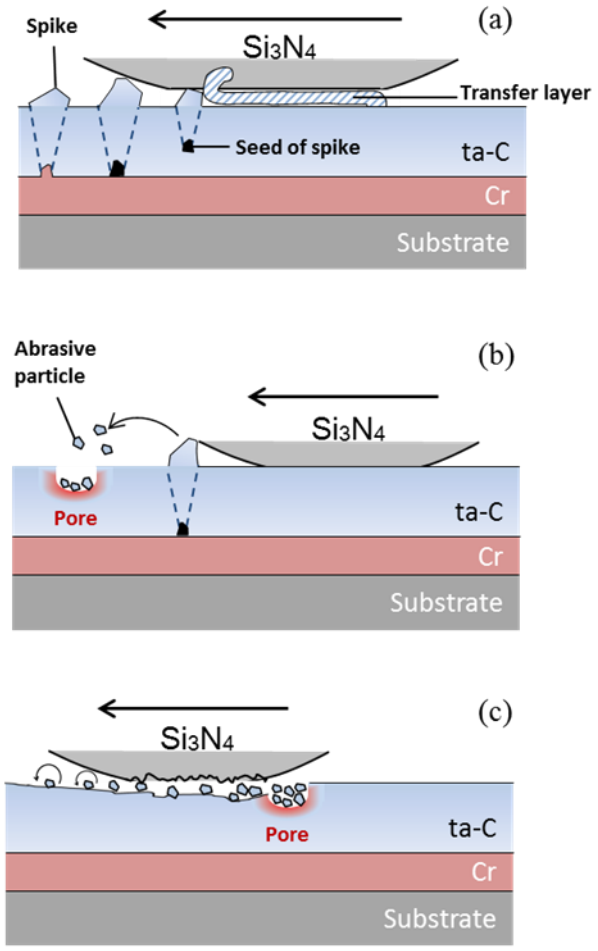

Figure 4.9. Wear mechanism was summarized like this. (a) peeling off transfer layer formed on counter-part material, (b) abrasive particle was provided by spikes of ta-C coating during the sliding and piled up at pore, (c) Pore was damaged by abrasive particle.

4.5 Conclusions

In this study, a ta-C coating was fabricated via FCVA. The observed defects in the ta-C coating were classified as droplets, pores, and spikes, according to their morphology, structure, and mechanical properties.

- Pores have low hardness and thermal resistance at high temperature. Spikes retains even after the friction test at 170 ℃.
- Droplets form concave pores
- During sliding, a tribolayer on the Si_3N_4 ball prevents to form the presence of spikes and droplets.
- Spalling of these spikes produced abrasive particles that caused severe wear at pores possessing a sp^2-rich structure and poor mechanical properties.

Chapter 5
Conclusions and future outlook

In this thesis, carbonaceous coatings with different structure and mechanical properties were deposited by FCVA methods. The thermal stability and high temperature tribological properties were investigated. From the tribological tests results and surface analysis, the main findings of this work can be summarized as follows:

(1) Deposition of ta-C coatings on Inconel disk with different substrate bias at 0, -100 and -300 V by FCVA system result to increases with the hardness, Young's modulus and sp^3 content estimated by I_D/I_G ratio increasing substrate bias to -100 V. Further increase of substrate bias upto -300 V, sp^3 structure changes to sp^2 structure decreases, consistently showed by Raman and nano-indentation test.

(2) The ta-C coatings on Inconel alloy substrates by FCVA with a different substrate bias of 0, 100 and 300 V has a higher sp^3 content and hardness than a-C and hydrogenated DLC. The applying substrate bias improves the mechanical and structural properties of ta-C. Hydrogen depletion occur at 100 ℃ and result in longer running-in cycles and the higher specific wear rate ($< 9\times10^{-6}$ mm^3/Nm). Steady state

friction coefficient decreased from 0.2 to 0.08 after formation of transfer layer. The wear rate was categorized into two distinct regions. In region Ⅰ at 23, 100 and 200 ℃, highest wear rate was shown at 100 ℃ where hydrogen depletion started to begin. Under these conditions, wear behaviors of 100 V ta-C coating show severe wear due to the abrasive particles with highest sp^3 content. In region Ⅱ at 300, 400 and 500 ℃, specific wear rate decreased with increasing substrate bias. Content of sp^3 was maintained in 100, 300 V ta-C coatings compared to 0 V ta-C coatings, which explain reduction of specific wear rate with an increase of substrate bias after 300 ℃.

(3) In the tribological behaviors of ta-C coating versus Si_3N_4 ball at high temperature as a function of sliding cycles, tribological behaviors at high temperature are affected by morphology of ta-C coating surface and transfer film formation. The running-in cycles shown up to 2000 cycles were finished with a removal of nodular defects and then specific wear rate was sharply decreased during the steady state region. Low friction coefficient of 0.02 and corresponding to lower wear rates of 2.5×10^{-7} mm^3/Nm are observed at 12000 cycles. Such a steady state friction coefficient and decrease of wear rate is attributed by the formation of transfer layer on the wear scar of the Si_3N_4 ball. This graphitized transfer layer around thickness of 300 nm can significantly protect the ta-C coating surface with covering whole area of Si_3N_4 surface. The results

demonstrate that transfer layer formation influence tribological behavior decreasing the interaction between ta-C films and wear scar on the Si_3N_4 sphere. Furthermore, higher wear rate was correlated with running-in cycles as a process of formations of carbonaceous transfer film.

(4) ta-C was fabricated by FCVA method. Some defect in ta-C coating was observed, these defects was divided by droplets, pores and spikes with a respect of morphological, structural and mechanical properties. In pore, it showed poor hardness and thermal resistance at high temperature. Especially, it is note that some of spikes were still remained during the friction test at 170 ℃ by comparison of surface morphology at designated area before and after tribological test. During the sliding, formation of tribo-layer on Si_3N_4 ball was prevented by the presence of spike. Spalled these spikes was a role of abrasive particle and result in severe wear at pore which had sp^2 rich structure and low mechanical properties.

Further study on effect of deposition parameter such as arc current, substrate bias and duct current on defect in ta-C coating need to be proven in appropriate future tests. In additional, future directions for this work would be to deposit ta-C coating with low number of defect, and investigate post-treatment to remove the defects and

promote to the formation of carbon transfer layer on counterpart material in high temperature condition, for industrial application.

References

[1] Stachowiak GW (Gwidon W. Wear--materials, mechanisms and practice. Wiley; 2005.

[2] Holmberg K, Andersson P, Erdemir A. Global energy consumption due to friction in passenger cars. Tribol Int 2012;47:221–34. doi:10.1016/J.TRIBOINT.2011.11.022.

[3] Kato K. Industrial Tribology in the Past and Future. Tribol Online 2011;6:1–9. doi:10.2474/trol.6.1.

[4] Hisakado T. Effect of surface roughness on contact between solid surfaces. Wear 1974;28:217–34. doi:10.1016/0043-1648(74)90163-X.

[5] Jiang J, Arnell R. The effect of substrate surface roughness on the wear of DLC coatings. Wear 2000;239:1–9. doi:doi: DOI: 10.1016/S0043-1648(99)00351-8.

[6] Bhushan B. Modern tribology handbook. CRC Press; 2001.

[7] Kato K. Wear in relation to friction — a review. Wear 2000;241:151–7. doi:10.1016/S0043-1648(00)00382-3.

[8] Singh H, Mutyala KC, Mohseni H, Scharf TW, Evans RD, Doll GL. Tribological Performance and Coating Characteristics of Sputter-Deposited Ti-Doped MoS_2 in Rolling and Sliding Contact. Tribol Trans 2015;58:767–77. doi:10.1080/10402004.2015.1015758.

[9] Donnet C, Erdemir A. Solid Lubricant Coatings: Recent Developments and Future Trends. Tribol Lett 2004;17:389–97. doi:10.1023/B:TRIL.0000044487.32514.1d.

[10] Donnet C, Erdemir A. Historical developments and new trends in tribological and solid lubricant coatings 2004;181:76–84. doi:10.1016/j.surfcoat.2003.10.022.

[11] Vanhulsel A, Velasco F, Jacobs R, Eersels L, Havermans D, Roberts EW, et al. DLC solid lubricant coatings on ball bearings for space applications. Tribol Int 2007;40:1186–94. doi:10.1016/j.triboint.2006.12.005.

[12] Space tribology. Nature 2005;255:194–5. doi:10.1038/255194b0.

[13] Briscoe HM. Why space tribology? Tribol Int 1990;23:67–74. doi:10.1016/0301-679X(90)90040-V.

[14] Shuo Zhang. Analysis of Phase Transitions and Crystal Structures of Novel Benzothiophene Derivatives. 2015. doi:10.13140.

[15] Grill A. Tribology of diamondlike carbon and related materials: An updated review. Surf Coatings Technol 1997;94–95:507–13. doi:10.1016/S0257-8972(97)00458-1.

[16] Vetter J. Surface & Coatings Technology 60 years of DLC coatings : Historical highlights and technical review of cathodic arc processes to synthesize various

DLC types , and their evolution for industrial applications. Surf Coat Technol 2014;257:213–40. doi:10.1016/j.surfcoat.2014.08.017.

[17] Zahid R, Masjuki • H H, Mahendra •, Riaz V•, Mufti A, Kalam MA, et al. Effect of Lubricant Formulations on the Tribological Performance of Self-Mated Doped DLC Contacts: a review n.d. doi:10.1007/s11249-015-0506-5.

[18] Tillmann W, Vogli E, Hoffmann F. Wear-resistant and low-friction diamond-like-carbon (DLC)-layers for industrial tribological applications under humid conditions. Surf Coatings Technol 2009;204:1040–5. doi:10.1016/j.surfcoat.2009.06.005.

[19] Robertson J. Mechanical properties and structure of diamond-like carbon. Diam Relat Mater 1992;1:397–406. doi:10.1016/0925-9635(92)90137-D.

[20] Moriguchi H, Ohara H, Tsujioka M. History and Applications of Diamond-Like Carbon Manufacturing Processes 1971:52–8.

[21] Hakovirta M, Tiainen V-M, Pekko P. Techniques for filtering graphite macroparticles in the cathodic vacuum arc deposition of tetrahedral amorphous carbon films. Diam Relat Mater 1999;8:1183–92. doi:10.1016/S0925-9635(99)00111-9.

[22] Rauthan CMS. Effect of hydrogen and nitrogen incorporation on the properties of tetrahedral amorphous carbon films grown using S bend filtered cathodic

vacuum arc process 2008;46:797–805.

[23] Bruno P, Cicala G, Losacco A., Decuzzi P. Mechanical properties of PECVD hydrogenated amorphous carbon coatings via nanoindentation and nanoscratching techniques. Surf Coatings Technol 2004;180–181:259–64. doi:10.1016/J.SURFCOAT.2003.10.035.

[24] Broitman E, Hellgren N, Wänstrand O, Johansson MP, Berlind T, Sjöström H, et al. Mechanical and tribological properties of CNx films deposited by reactive magnetron sputtering. Wear 2001;248:55–64. doi:10.1016/S0043-1648(00)00519-6.

[25] Ferrari AC, Robertson J. Interpretation of Raman spectra of disordered and amorphous carbon. Phys Rev B 2000;61:14095–107. doi:10.1103/PhysRevB.61.14095.

[26] Hauert R. An overview on the tribological behavior of diamond-like carbon in technical and medical applications. Tribol Int 2004;37:991–1003. doi:10.1016/j.triboint.2004.07.017.

[27] Grill A. Diamond-like carbon: state of the art. Diam Relat Mater 1999;8:428–34. doi:10.1016/S0925-9635(98)00262-3.

[28] Ronkainen H, Varjus S, Koskinen J, Holmberg K. Differentiating the tribological performance of hydrogenated and hydrogen-free DLC coatings.

Wear 2001;249:260–6. doi:10.1016/S0043-1648(01)00558-0.

[29] Koskinen J, Schneider D, Ronkainen H, Muukkonen T, Varjus S, Burck P, et al. Microstructural changes in DLC films due to tribological contact. Surf Coatings Technol 1998;108–109:385–90. doi:10.1016/S0257-8972(98)00656-2.

[30] Robertson J. Comparison of diamond-like carbon to diamond for applications. Phys Status Solidi Appl Mater Sci 2008;205:2233–44. doi:10.1002/pssa.200879720.

[31] Overview of Amorphous Carbon Films 2017. doi:10.1007/978-981-10-4882-1.

[32] Erdemir A, Donnet C. Tribology of diamond-like carbon films: Recent progress and future prospects. J Phys D Appl Phys 2006;39. doi:10.1088/0022-3727/39/18/R01.

[33] Khurshudov AG, Kato K. Tribological properties of carbon nitride overcoat for thin-film magnetic rigid disks. Surf Coatings Technol 1996;86–87:664–71. doi:10.1016/S0257-8972(96)03072-1.

[34] Fernández A, Fernández-Ramos C, Sánchez-López J. Preparation, microstructural characterisation and tribological behaviour of CNx coatings. Surf Coatings Technol 2003;163–164:527–34. doi:10.1016/S0257-8972(02)00615-1.

[35] Access O. New application perspective for tetrahedral amorphous carbon

coatings n.d.

[36] Lopez S, Dunlop HM, Benmalek M, Tourillon G, Wong M-S, Sproul WD. XPS, XANES and ToF-SIMS Characterization of Reactively Magnetron-sputtered Carbon Nitride Films. Surf Interface Anal 1997;25:827–35. doi:10.1002/(SICI)1096-9918(199709)25:10<827::AID-SIA331>3.0.CO;2-W.

[37] Schmidt S, Czigány Z, Wissting J, Greczynski G, Janzén E, Jensen J, et al. A comparative study of direct current magnetron sputtering and high power impulse magnetron sputtering processes for CNx thin film growth with different inert gases. Diam Relat Mater 2016;64:13–26. doi:10.1016/J.DIAMOND.2016.01.009.

[38] Schwan J, Ulrich S, Roth H, Ehrhardt H. Tetrahedral amorphous carbon films prepared by magnetron sputtering and dc ion plating 1996;79.

[39] Boyd KJ, Marton D, Todorov SS, Al‐Bayati AH, Kulik J, Zuhr RA, et al. Formation of C–N thin films by ion beam deposition. J Vac Sci Technol A Vacuum, Surfaces, Film 1995;13:2110–22. doi:10.1116/1.579528.

[40] Voevodin AA, Jones JG, Back TC, Zabinski JS, Strel'nitzki VE, Aksenov II. Comparative study of wear-resistant DLC and fullerene-like CNx coatings produced by pulsed laser and filtered cathodic arc depositions. Surf Coatings Technol 2005;197:116–25. doi:10.1016/J.SURFCOAT.2004.06.021.

[41] Zheng X, Yang F, Chen L, Chen Z, Song R, Zhang X. Microstructure and mechanical properties of a-CNx films prepared by bias voltage assisted PLD with carbon nitride target. Surf Coatings Technol 2014;258:716–21. doi:10.1016/J.SURFCOAT.2014.08.009.

[42] Polo MC, Andújar JL, Hart A, Robertson J, Milne WI. Preparation of tetrahedral amorphous carbon films by filtered cathodic vacuum arc deposition. Diam Relat Mater 2000;9:663–7. doi:10.1016/S0925-9635(99)00339-8.

[43] Aksenov II, Strel'nitskij VE. Properties of diamond-like coatings prepared by vacuum arc deposition. Surf Coatings Technol 1991;47:98–105. doi:10.1016/0257-8972(91)90272-X.

[44] Kang MC, Tak HS, Jeong YK, Lee HW, Kim JS. Properties and tool performance of ta-C films deposited by double-bend filtered cathodic vacuum arc for micro drilling applications. Diam Relat Mater 2010;19:866–9. doi:10.1016/J.DIAMOND.2010.02.002.

[45] Murata Y, Choo C-K, Ono H, Nagai Y, Tanaka K. Characterization of N-doped DLC Thin Films Prepared by Hydrocarbons Pyrolysis Method. Mater Today Proc 2016;3:S197–202. doi:10.1016/J.MATPR.2016.02.033.

[46] Chen CW, Robertson J. Doping mechanism in tetrahedral amorphous carbon. Carbon N Y 1999;37:839–42. doi:10.1016/S0008-6223(98)00281-4.

[47] McCann R, Roy SS, Papakonstantinou P, Abbas G, McLaughlin JA. The effect of thickness and arc current on the structural properties of FCVA synthesised ta-C and ta-C:N films. Diam Relat Mater 2005;14:983–8. doi:10.1016/J.DIAMOND.2004.12.037.

[48] Ferrari AC. Determination of bonding in diamond-like carbon by Raman spectroscopy. Diam Relat Mater 2002;11:1053–61. doi:10.1016/S0925-9635(01)00730-0.

[49] Yang Mingchu, Zhang Mingsheng, Zhao Jinmin, Liu Bo. Nitrogen doping in tetrahedral carbon and its effect on lubricant bonding. 2009 Asia-Pacific Magn. Rec. Conf., IEEE; 2009, p. 1–2. doi:10.1109/APMRC.2009.4925362.

[50] Filtered cathodic arc source 1996.

[51] Andujar JL, Polo MC, Esteve J, Robertson J, Milne WI, Martínez E. Study of the mechanical properties of tetrahedral amorphous carbon films by nanoindentation and nanowear measurements. Diam Relat Mater 2001;10:145–52. doi:10.1016/S0925-9635(00)00461-1.

[52] Zhang G, Yan P, Wang P, Chen Y, Zhang J, Wang L, et al. The effect of applied substrate negative bias voltage on the structure and properties of Al-containing a-C:H thin films. Surf Coatings Technol 2008;202:2684–9. doi:10.1016/j.surfcoat.2007.09.051.

[53] Deng X, Kousaka H, Tokoroyama T, Umehara N. Tribological behavior of tetrahedral amorphous carbon (ta-C) coatings at elevated temperatures. Tribol Int 2014;75:98–103. doi:10.1016/j.triboint.2014.04.002.

[54] Kalish R, Lifshitz Y, Nugent K, Prawer S. Thermal stability and relaxation in diamond-like-carbon. A Raman study of films with different sp3fractions (ta-C to a-C). Appl Phys Lett 1999;74:2936–8. doi:10.1063/1.123971.

[55] Bhowmick S, Banerji A, Khan MZU, Lukitsch MJ, Alpas AT. Surface & Coatings Technology High temperature tribological behavior of tetrahedral amorphous carbon (ta-C) and fl uorinated ta-C coatings against aluminum alloys. Surf Coat Technol 2015;284:14–25. doi:10.1016/j.surfcoat.2015.08.071.

[56] Bhowmick S, Banerji A, Khan MZU, Lukitsch MJ, Alpas AT. High temperature tribological behavior of tetrahedral amorphous carbon (ta-C) and fluorinated ta-C coatings against aluminum alloys. Surf Coatings Technol 2015;284:14–25. doi:10.1016/j.surfcoat.2015.08.071.

[57] Tay B., Shi X, Tan H., Yang H., Sun Z. Raman studies of tetrahedral amorphous carbon films deposited by filtered cathodic vacuum arc. Surf Coatings Technol 1998;105:155–8. doi:10.1016/S0257-8972(98)00475-7.

[58] Zavaleyev V, Walkowicz J. Influence of the substrate bias potential on the properties of ta-C coatings deposited using Venetian blind plasma filter. Thin

Solid Films 2015;581:32–8. doi:10.1016/J.TSF.2014.11.074.

[59] Robertson J. Diamond-like amorphous carbon. Mater Sci Eng R Reports 2002;37:129–281. doi:10.1016/S0927-796X(02)00005-0.

[60] Jang YJ, Kang YJ, Kitazume K, Umehara N, Kim J. Mechanical and electrical properties of micron-thick nitrogen-doped tetrahedral amorphous carbon coatings. Diam Relat Mater 2016;69:121–6. doi:10.1016/j.diamond.2016.08.001.

[61] Guo CQ, Pei ZL, Fan D, Gong J, Sun C. Microstructure and tribomechanical properties of (Cr, N)-DLC/DLC multilayer films deposited by a combination of filtered and direct cathodic vacuum arcs. Diam Relat Mater 2015;60:66–74. doi:10.1016/j.diamond.2015.10.019.

[62] Takikawa H. Review of cathodic arc deposition for preparing droplet-free thin films. Proc - Int Symp Discharges Electr Insul Vacuum, ISDEIV 2006;2:525–30. doi:10.1109/DEIV.2006.357354.

[63] Teo KBK, Rodil SE, Tsai JTH, Ferrari AC, Robertson J, Milne WI. Effect of graphitic inclusions on the optical gap of tetrahedral amorphous carbon films. J Appl Phys 2001;89:3706–10. doi:10.1063/1.1351863.

[64] Takikawa H, Izumi K, Miyano R, Sakakibara T. DLC thin film preparation by cathodic arc deposition with a super droplet-free system. Surf Coatings Technol

2003;163–164:368–73. doi:10.1016/S0257-8972(02)00629-1.

[65] Takikawa H, Tanoue H. Review of Cathodic Arc Deposition for Preparing Droplet-Free Thin Films. IEEE Trans Plasma Sci 2007;35:992–9. doi:10.1109/TPS.2007.897907.

[66] Mabuchi Y, Higuchi T, Inagaki Y, Kousaka H, Umehara N. Wear analysis of hydrogen-free diamond-like carbon coatings under a lubricated condition. Wear 2013;298–299:48–56. doi:10.1016/j.wear.2012.11.046.

[67] Sheeja DU, Tay BK, Lau SP, Shi X, Ding X. Structural and tribological characterization of multilayer ta-C films prepared by filtered cathodic vacuum arc with substrate pulse biasing 2000:228–32.

[68] Waesche R, Hartelt M, Weihnacht V. Influence of counterbody material on wear of ta-C coatings under fretting conditions at elevated temperatures. Wear 2009;267:2208–15. doi:10.1016/j.wear.2009.08.041.

[69] Robertson J. Hard amorphous (diamond-like) carbons. Prog Solid State Chem 1991;21:199–333. doi:10.1016/0079-6786(91)90002-H.

[70] Koidl P, Wild C, Dischler B, Wagner J, Ramsteiner M. Plasma Deposition, Properties and Structure of Amorphous Hydrogenated Carbon Films. Mater Sci Forum 1991;52–53:41–70. doi:10.4028/www.scientific.net/MSF.52-53.41.

[71] Mróz W, Burdyńska S, Prokopiuk A, Jedyński M, Budner B. Characteristics of

Carbon Films Deposited by Magnetron Sputtering 2009;116:120–2.

[72] Miyoshi K, Pohlchuck B, Street KW, Zabinski J., Sanders J., Voevodin A., et al. Sliding wear and fretting wear of diamondlike carbon-based, functionally graded nanocomposite coatings. Wear 1999;225–229:65–73. doi:10.1016/S0043-1648(98)00349-4.

[73] Siegal MP, Martinez-Miranda LJ, DiNardo NJ, Tallant DR, Barbour JC, Newcomer Provencio P. <title>Characterization of amorphous carbon films grown by pulsed laser deposition</title> In: Phipps CR, editor., 1998, p. 885–94. doi:10.1117/12.321617.

[74] Iijima Y, Harigai T, Isono R, Imai T, Suda Y, Takikawa H, et al. Fabrication of nitrogen-containing diamond-like carbon film by filtered arc deposition as conductive hard-coating film n.d.

[75] Boxman RL, Zhitomirsky V, Alterkop B, Gidalevich E, Beilis I, Keidar M, et al. Recent progress in filtered vacuum arc deposition. Surf Coatings Technol 1996;86–87:243–53. doi:10.1016/S0257-8972(96)03023-X.

[76] Engineering S. Unfiltered and filtered cathodic arc deposition. 2016. doi:10.1016/B978-0-8155-2031-3.00010-7.

[77] Kamiya M, Tanoue H, Takikawa H, Taki M, Hasegawa Y, Kumagai M. Preparation of various DLC films by T-shaped filtered arc deposition and the

effect of heat treatment on film properties. Vacuum 2008;83:510–4. doi:10.1016/j.vacuum.2008.04.016.

[78] Kamiya M, Tanoue H, Takikawa H, Taki M. Preparation of various DLC films by T-shaped filtered arc deposition and the effect of heat treatment on film properties 2009;83:510–4. doi:10.1016/j.vacuum.2008.04.016.

[79] Konkhunthot N, Euaruksakul C, Photongkam P, Wongpanya P. Characterization of Diamond-like Carbon (DLC) Films Deposited by Filtered Cathodic Vacuum arc Technique. J Met Mater Miner 2013;23:35–40.

[80] Polo MC, Andú Jar JL, Hart A, Robertson J, Milne WI. Preparation of tetrahedral amorphous carbon films by filtered cathodic vacuum arc deposition. Diam Relat Mater 2000;9:663–7. doi:10.1016/S0925-9635(99)00339-8.

[81] Sheeja D, Tay BK, Lau SP, Shi X, Ding X. Structural and tribological characterization of multilayer ta-C films prepared by filtered cathodic vacuum arc with substrate pulse biasing. Surf Coatings Technol 2000;132:228–32. doi:10.1016/S0257-8972(00)00848-3.

[82] Murakawa M, Takeuchi S. Evaluation of tribological properties of DLC films used in sheet forming of aluminum sheet. Surf Coatings Technol 2003;163–164:561–5. doi:10.1016/S0257-8972(02)00624-2.

[83] Robertson J. Diamond-like amorphous carbon 2002;37:129–281.

doi:10.1016/S0927-796X(02)00005-0.

[84] Wang J, Pu J, Zhang G, Wang L. Tribology International Architecture of superthick diamond-like carbon fi lms with excellent high temperature wear resistance. Tribiology Int 2015;81:129–38. doi:10.1016/j.triboint.2014.08.017.

[85] Banerji A, Bhowmick S, Alpas AT. High temperature tribological behavior of W containing diamond-like carbon (DLC) coating against titanium alloys. Surf Coatings Technol 2014;241:93–104. doi:10.1016/j.surfcoat.2013.10.075.

[86] Gharam AA, Lukitsch MJ, Balogh MP, Alpas AT. High temperature tribological behaviour of carbon based (B 4 C and DLC) coatings in sliding contact with aluminum. Thin Solid Films 2010;519:1611–7. doi:10.1016/j.tsf.2010.07.074.

[87] Konca E, Cheng YT, Weiner AM, Dasch JM, Alpas AT. Elevated temperature tribological behavior of non-hydrogenated diamond-like carbon coatings against 319 aluminum alloy. Surf Coatings Technol 2006;200:3996–4005. doi:10.1016/j.surfcoat.2005.02.202.

[88] Vetter J. 60years of DLC coatings: Historical highlights and technical review of cathodic arc processes to synthesize various DLC types, and their evolution for industrial applications. Surf Coatings Technol 2014;257:213–40. doi:10.1016/j.surfcoat.2014.08.017.

[89] Drescher D, Scheibe HJ, Mensch A, Alers P, Dyer C. Morphology and structural

characterization of plasma-assisted prepared carbon films. Diam Relat Mater 1996;5:968–72. doi:10.1016/0925-9635(95)00438-6.

[90] Ferrari AC, Robertson J, Robertson J. Interpretation of Raman spectra of disordered and amorphous carbon. Phys Rev B 2000;61:14095–107. doi:10.1103/PhysRevB.61.14095.

[91] Marino MJ, Hsiao E, Chen Y, Eryilmaz OL, Erdemir A, Kim SH. Understanding Run-In Behavior of Diamond-Like Carbon Friction and Preventing Diamond-Like Carbon Wear in Humid Air 2011:12702–8. doi:10.1021/la202927v.

[92] Donnet C, Fontaine J, Grill A, Mogne T Le. The role of hydrogen on the friction mechanism of diamond-like carbon films 2001;9:137–42.

[93] Qin W, Wang C. RSC Advances Understanding integrated e ff ects of humidity and interfacial transfer fi lm formation on tribological behaviors of sintered polycrystalline diamond. RSC Adv 2015;5:53484–96. doi:10.1039/C5RA09327A.

[94] Dorner A, Schürer C, Reisel G, Irmer G, Seidel O, Müller E. Diamond-like carbon-coated Ti6Al4V: influence of the coating thickness on the structure and the abrasive wear resistance. Wear 2001;249:489–97. doi:10.1016/S0043-1648(01)00587-7.

[95] Enke K, Dimigen H, Hübsch H. Frictional properties of diamondlike carbon layers. Appl Phys Lett 1980;36:291–2. doi:10.1063/1.91465.

[96] Holmberg K, Ronkainen H, Matthews A. Tribology of thin coatings. Ceram Int 2000;26:787–95. doi:10.1016/S0272-8842(00)00015-8.

[97] Robertson J. Amorphous carbon. Adv Phys 1986;35:317–74. doi:10.1080/00018738600101911.

[98] Ronkainen H, Holmberg K. Environmental and thermal effects on the tribological performance of DLC coatings. Tribol Diamond-Like Carbon Film Fundam Appl 2008:155–200. doi:10.1007/978-0-387-49891-1_6.

[99] Sheeja D, Tay BK, Krishnan SM, Nung LN. Tribological characterization of diamond-like carbon (DLC) coatings sliding against DLC coatings. Diam Relat Mater 2003;12:1389–95. doi:10.1016/S0925-9635(03)00165-1.

[100] Sheeja D, Tay BK, Lau SP, Shi X. Tribological properties and adhesive strength of DLC coatings prepared under different substrate bias voltages. Wear 2001;249:433–9. doi:http://dx.doi.org/10.1016/S0043-1648(01)00541-5.

[101] Donnet C, Grill A, Fontaine J, Le Mogne T, Lefebvre F, Patel V, et al. Fundamentals on the friction mechanism of diamondlike carbon films. Tribol Ser 1999;36:137–42. doi:http://dx.doi.org/10.1016/S0167-8922(99)80054-6.

[102] Vetter J, Stuber M, Ulrich S. Growth effects in carbon coatings deposited by

magnetron sputtering. Surf Coatings Technol 2003;168:169–78. doi:10.1016/S0257-8972(03)00010-0.

[103] Panjan P, Gselman P, Kek-Merl D, Čekada M, Panjan M, Dražić G, et al. Growth defect density in PVD hard coatings prepared by different deposition techniques. Surf Coatings Technol 2013;237:349–56. doi:10.1016/j.surfcoat.2013.09.020.

Acknowledgements

First of all, I would like to express my sincere gratitude and respect to my supervisor, Prof. Dr. Noritsugu Umehara, for all I have learned from him and for his excellent guidance, continuous help, patience, motivation and support in all stages of this thesis. I would also like to thank him for being an open person to ideas, and for encouraging and helping me to shape my interest and ideas. Without his guidance and persistent help this dissertation would not have been possible.

I would like to thank my committee members, Prof. Dr. Seiichi Hata, Appointed Prof. Dr. Kenji Ishikawa and Assoc. Prof. Dr. Takayuki Tokoroyama for sharing their ideas on the improvement of the thesis, and for their encouragement, insightful comments, and suggestions.

The success of this thesis is attributed to the extensive support and assistance from all members of Advanced Material and Manufacturing Laboratory. Especially, I would like to express my grateful gratitude and sincere appreciation to Assist. Prof. Dr. Motoyuki Murashima and Mr. Shinkoh Senda for their kindness in examining the research work and providing technical suggestions for improvement and encouragement during my time here.

My special thanks are given to my lab members for his cheerful cooperation, encouragement, help and support and enjoyment during the course of my study, Dr.Liu, Mr. Taufik, and Mr. Melardot and all others who I can't write their name in here. I hope our friendship will remain same in coming years. In particular, I would like to thank for Dr. Jang Young-Jun and KIMS members.

I would also like to express my special thanks to my family, especially Lee Jong-Ha and my parents for always believing in me, for their continuous love and their supports in my decisions. I am particularly grateful for the support, love and good times given by all my relatives and friend. They were always there cheering me up, praying for my health and stood by me through the good times and bad. Without whom I could not have made it here.

Publication list

International Journal:

- **Lee, W.Y.**, Tokoroyama, T., Jang, Y.J., Umehara, N., Effect of substrate bias and temperature on friction and wear properties for ta-C coating prepared under different substrate bias voltages with filtered cathodic vacuum arc deposition. *Tribology online*, Vol.13, No.5, pp.241-247 (2018).

- **Lee, W.Y.**, Tokoroyama, T., Jang, Y.J., Murashima M., Umehara, N., Investigating running-in behavior to understand wear behavior of ta-C coating with filtered cathodic vacuum arc deposition. *Jurnal tribologi* (2019, accepted for publication)

International Conference:

- **Lee, W.Y.**, Umehara, N., Tokoroyama, T., Murashima M., Jang, Y.J., KIM, J.K. Tribological study of thick ta-C coating at elevated temperatures prepared under different substrate bias voltages, 6th World Tribology Conference(WTC), Beijing (China), Sep., 2017.

- **Lee, W.Y.**, Tokoroyama, T., Murashima M., Jang, Y.J., KIM, J.K., Umehara, N. Investigating run-in behavior of ta-C friction and understating wear behavior at high temperature, 6th ASIATRIB, SRAWAK (Malaysian), Sep., 2018.

- **Lee, W.Y.**, Tokoroyama, T., Murashima M., Jang, Y.J., Umehara, N. Understanding formation and growth of transfer layer of ta-C coating deposited by FCVA technique, 8th International Conference on Manufacturing, Machine Design and Tribology (ICMDT), Kagoshima (Japan), April., 2019.